

1 Title page

2
3 **Bax-derived membrane active peptides act as potent and direct inducers of apoptosis in**
4 **cancer cells**
5

6 Juan GARCIA VALERO ¹, Lucie SANCEY ², Jérôme KUCHARCZAK ¹, Yannis
7 GUILLEMIN ¹, Diana GIMENEZ ³, Julien PRUDENT ¹, Germain GILLET ¹, Jesús
8 SALGADO ^{3,4}, Jean-Luc COLL ² and Abdel AOUACHERIA ^{1¶}
9

10 ¹ IBCP, Institut de Biologie et Chimie des Protéines, 7 passage du Vercors, Lyon, F-69367,
11 France ; CNRS, UMR 5086 ; Université de Lyon, France ; Université Lyon 1, France ; IFR
12 128, Lyon, France ;

13 ² CRI-INSERM-UJF U823, institut Albert-Bonniot, université Joseph-Fourier, BP 170, La
14 Tronche, 38042 Grenoble cedex 9, France ;

15 ³ Instituto de Ciencia Molecular, Universidad de Valencia, Polígono La Coma, s/n, 46980
16 Paterna (Valencia) España ;

17 ⁴ Departamento de Bioquímica y Biología Molecular, Universidad de Valencia, C/ Doctor
18 Moliner, 50, 46100 Burjassot (Valencia) España.
19

20
21 ¶ To whom correspondence should be addressed. IBCP, CNRS UMR 5086, 7 passage du
22 Vercors, F-69367 LYON Cedex France. Tel: +33-472-72-26-11; Fax: +33-472-72-26-01; e-
23 mail: a.aouacheria@ibcp.fr
24

25 Running title: Cytotoxic effects of Bax peptides
26
27

SUMMARY

Although many cancer cells are primed for apoptosis, they usually develop resistance to cell death at multiple levels. Permeabilization of the outer mitochondrial membrane, which is mediated by proapoptotic Bcl-2 family members like Bax, is considered as a point-of-no-return for initiating apoptotic cell death. This crucial role has placed Bcl-2 family proteins as recurrent targets for anticancer drug development. Here, we propose and demonstrate a new concept based on using minimal active version of Bax to induce cell death independently of endogenous Bcl-2 proteins. We show that membrane-active segments of Bax can directly induce the release of mitochondria-residing apoptogenic factors and commit tumor cells promptly and irreversibly to caspase-dependent apoptosis. On this basis, we designed a peptide encompassing part of the Bax pore-forming domain, able to target mitochondria, induce cytochrome c release and trigger caspase-dependent apoptosis. Moreover, this Bax-derived 'poropeptide' produced effective tumor regression after peritumoral injection in a nude mouse xenograft model. Thus, peptides derived from proteins evolutionary functionalized to form pores in the mitochondrial outer membrane represent novel templates for anticancer agents.

Keywords: Cytotoxicity / anticancer activity /apoptosis /Bcl-2 family / mitochondria / pore-forming peptides / proapoptotic Bax

1 INTRODUCTION

2
3 The integrity of the mitochondrial outer membrane (MOM) serves as a switch between cell
4 survival and cell death by apoptosis. The Bcl-2 family of proteins are critical arbiters in this
5 process due to their ability to either promote or inhibit MOM permeabilization (Aouacheria et
6 al., 2007; Youle and Strasser, 2008). Pro-apoptotic members (e.g. Bax, Bak, BH3-only
7 proteins) promote cytochrome c release from mitochondria, leading to the activation of
8 proteases termed caspases that mediate cell demise. Conversely, anti-apoptotic members such
9 as Bcl-2 or Bcl-xL decrease cell death susceptibility by neutralizing Bax/Bak or BH3-only
10 proteins.

11 Over-expression of pro-survival proteins occurs in many human tumors, and can contribute
12 not only to disease development and progression but also to clinical drug resistance (Adams
13 and Cory, 2007). Anti-apoptotic Bcl-2 family members therefore represent prime targets for
14 the development of modern anticancer drugs that have the potential to restore apoptosis and
15 reverse resistance to chemotherapy. Efforts to inhibit the anti-death Bcl-2 family members
16 have focused on the development of cell-permeable peptides or small-molecule inhibitor
17 drugs, designed to mimic the BH3 domain of Bcl-2 family death members (Yip and Reed,
18 2008). A number of such BH3 mimics (e.g. ABT-737) (Oltersdorf et al., 2005), which
19 inactivate Bcl-2-like proteins by binding to their BH3-binding groove, have now entered
20 clinical trials and provide real opportunities for improving the efficacy of cancer treatment.
21 Recently, another strategy has been described that converts pro-survival Bcl-2 molecules into
22 pro-apoptotic proteins with the potential to kill cancer cells. In this new approach, a short
23 peptide derived from the orphan nuclear receptor Nur77 was shown to bind to the N-terminal
24 regulatory region of Bcl-2, altering its structure to expose its BH3 domain, which then
25 becomes free to activate Bax/Bak (Kolluri et al., 2008). However, one major common
26 limitation of these two latter strategies is that they depend on endogenous levels of anti-
27 apoptotic Bcl-2 proteins in cancer cells. Moreover, these strategies are expected to be less
28 effective in inducing apoptosis of tumor cells with mutated or deficient Bax or Bak (Jansson
29 and Sun, 2002; Ouyang et al., 1998; Zong et al., 2001).

30 While apoptosis signaling pathways are often compromised during malignant transformation,
31 mitochondria-resided apoptogenic factors are still present in cancer cells and it is an exciting
32 challenge to develop peptides or peptidomimetics capable of inducing their release. Such
33 molecules would have the capacity to promote MOM permeabilization directly, and thus to
34 overcome cancer cell resistance towards apoptosis induction. Furthermore, molecules that

function at the membrane level are less likely to encounter resistance than drugs based on classical ‘lock-and-key’ binding specificity. Following these ideas, it has been shown in several studies that, upon cell internalization, antimicrobial peptides (e.g. (KLAKLAK)₂) can induce cell death in a variety of cell types (Chen et al., 2001; Ellerby et al., 1999; Foillard et al., 2008; Foillard et al., 2009; Law et al., 2006; Mai et al., 2001; Marks et al., 2005; Rege et al., 2007). However, the mechanisms of cell killing exerted by these antibiotic peptides are unclear, as they appear to include both necrosis, secondary to plasma membrane disruption (Papo et al., 2006), and apoptosis induced either by upregulation of death effectors (Chen et al., 2001) or by mitochondrial membrane permeabilization (Ellerby et al., 1999; Law et al., 2006; Mai et al., 2001; Marks et al., 2005; Rege et al., 2007). Noteworthy, the cationic peptide (KLAKLAK)₂ has been reported to have very low potency (Borgne-Sanchez et al., 2007; Ellerby et al., 1999), which precludes its use as an effective anticancer drug.

In this context, it is an important goal to identify novel pro-apoptotic sequences, acting directly at the level of mitochondrial permeability, which can be exploited to engineer potent anticancer molecules. Among the potential candidates are membranolytic peptides derived from proapoptotic Bcl-2 family proteins such as Bax. This 23-kD protein contains a number of structurally defined membrane-interacting regions (Suzuki et al., 2000), some of them (α 1, α 9, α 5, α 6 and a central α 5 α 6-hairpin motif) with a presumed membrane-targeting function (Annis et al., 2005; Cartron et al., 2005; Garcia-Saez et al., 2004; Heimlich et al., 2004). It has been previously shown that peptides corresponding to the first and/or to the second helix of the putative pore-forming domain of Bax (α 5- α 6 hairpin) can reproduce, at least in part, the poration activity displayed by the full-length parent protein (Garcia-Saez et al., 2005; Garcia-Saez et al., 2006; Guillemain et al.). Hence, helices α 5- α 6 of Bax carry by themselves minimal structural information and physicochemical properties to insert into model lipid membranes and form pores. The pores appear to be of the mixed lipidic-peptidic type (Garcia-Saez et al., 2007; Qian et al., 2008), similar to those of membrane-active, amphipathic peptide antibiotics (Fuentes et al., 2010). Here, we report that the two central helices of Bax individually are sufficient to target GFP to mitochondria and induce caspase-dependent cell death. Moreover, we demonstrate that a peptide designed from helix 5 can induce directly the release of mitochondrial cytochrome c, thereby acting as a potent apoptosis activator. This peptide, named ‘poropeptide-Bax[106-134]’, was more efficient for both mitochondrial targeting and apoptosis induction than (KLAKLAK)₂, a *de novo* synthetic peptide. Finally, we report a clear anticancer effect of poropeptide-Bax[106-134] after peritumoral administration in tumor-

bearing mice. Our data establish the feasibility of using short peptides derived from mitochondrial outer membrane-porating proteins as a basis for designing novel anticancer agents, which may be directly applied to some solid tumors or ‘homed’ to the tumor microenvironment through the use of specific vectors.

RESULTS

Bax- α 5/ α 6-containing constructs induce caspase-dependent apoptosis in transfected cells

In a search for peptide sequences capable of targeting and disrupting the MOM, recombinant constructs encoding the GFP open reading frame fused to the N-terminus of various membrane-active fragments of Bax (α 1, α 9, α 5, α 6, α 5 α 6 and α 5- α 9) were prepared (see definition of fragments and schemes of constructs in Fig. 1A). Western blot analysis confirmed the correct size of the fusion proteins (Fig. 1B, upper panel). The different constructs were transfected into human HT1080 cells and cell death was measured after 24h. As a measure of cell viability, GFP-positive cells were analyzed by Annexin V staining (Fig. 1C) or scored for nuclear apoptosis (as assessed by morphology) or necrosis (by staining with propidium iodide) (Fig. S1, top and middle). GFP alone, GFP-Bax and GFP-Bax- α 1 had no cytotoxic effect. The other constructs were all able to induce predominantly apoptotic cell death, with maximum activity observed after transfection with GFP-Bax- α 5 α 6, GFP-Bax- α 5 and GFP-Bax- α 6, and intermediate levels for GFP-Bax- α 5- α 9 and GFP-Bax- α 9. Furthermore, fusion proteins including the α 5 and/or α 6 helices of Bax elicited caspase-3 and PARP cleavage, as evidenced by western blot (Fig. 1B, bottom and middle panels, respectively). Consistently, treatment with 100 μ M zVAD.fmk, a cell-permeable caspase inhibitor, was effective in reducing cell death induced by the toxic GFP fusion proteins (Fig. S1, middle), indicating that cell death is caspase-dependent. Importantly, the pro-apoptotic effects of the Bax-derived constructs were not exerted through Bax and Bak, because Bax/Bak double knockout MEFs (MEF DKO) were as sensitive as wild-type MEFs to Bax- α 5 expression (Fig. S1, bottom), while being resistant to staurosporine treatment (Fig. 1D).

Fusions including Bax- α 5/ α 6 localize to mitochondria and alter the organelle physiology

1 The subcellular localization of all assayed GFP-tagged Bax fragments was subsequently
2 evaluated by confocal fluorescence microscopy. Expression of the fusion proteins yielded
3 abundant and intense GFP fluorescence in transfected MEF-DKO cells (Fig. 2). GFP alone
4 showed a diffuse localization. Similarly, GFP-Bax and GFP-Bax- α 1 distributed evenly
5 between the nuclear and cytoplasmic compartments in transfected cells. In contrast, confocal
6 imaging revealed that GFP-Bax- α 5, GFP-Bax- α 6, GFP-Bax- α 5 α 6, GFP-Bax- α 5- α 9 and
7 GFP-Bax- α 9 exhibited a clustered staining, reminiscent of intracellular membranes. The
8 simultaneous use of a mitochondrion-specific red marker (mitoDsRed) indicated that this
9 punctuated staining colocalized with mitochondria. This was confirmed by immunostaining of
10 GFP-Bax- α 5-transfected cells using anti-mitoHsp70, which shows that a large portion of the
11 fusion protein is indeed specifically associated with mitochondria (Fig. 2, bottom). Of note,
12 GFP-Bax- α 5 was also found to be more efficient for mitochondrial targeting than a fusion
13 containing the sequence of the designed proapoptotic peptide (KLAKLAK)₂ (Fig. 2).

15 Mitochondria dependent apoptosis typically affects the homeostasis of the organelle, which
16 can be investigated by tracing changes of the mitochondrial membrane potential $\Delta\Psi$ m. Thus,
17 using the membrane-potential sensitive dye Mitotracker Red CMXRos, we measured $\Delta\Psi$ m in
18 cells expressing either MOM-targeting sequences (GFP-Bax- α 5, GFP-Bax- α 6, GFP-Bax-
19 α 5 α 6, GFP-Bax- α 5- α 9 and GFP-Bax- α 9) or non-targeting sequences (GFP and GFP-Bax-
20 α 1). Examination of individual cells showed that those having strong expression of the
21 cytotoxic, MOM-targeting GFP-tagged fusions exhibited a concomitant decrease of
22 Mitotracker Red staining (Fig. 3 and Fig. S2, top panel), meaning a loss of the mitochondrial
23 membrane permeability. Analysis of $\Delta\Psi$ m changes by FACS yielded comparable results (Fig.
24 S2, middle and bottom), with values correlating with the apoptotic activity.

26 From the experiments described so far, we can conclude that the sequences from the central
27 hairpin of Bax as well as the Bax TM domain (α 9) contain the necessary information to target
28 the GFP protein specifically to the mitochondrial membranes. However, the Bax- α 5- or Bax-
29 α 6-containing chimeras distinguish themselves from the GFP-Bax- α 9 fusion by being
30 markedly more active for inducing depolarization of the mitochondrial membrane and
31 caspase-dependent apoptosis. Both Bax- α 5 and Bax- α 6, either in the Bax protein (Suzuki et
32 al., 2000) or as individual peptides bound to membranes (Garcia-Saez et al., 2005; Garcia-
33 Saez et al., 2006) form amphipathic α -helices. Additionally, they have a similar ratio of

hydrophilic to hydrophobic residues (31% and 33%, respectively). However, the expected net charge of these fragments is very different at neutral pH, namely: +4 for Bax- α 5 and -1 for Bax- α 6, indicating that Bax- α 5 is a better candidate for binding and disruption of the mitochondrial outer membrane, rich in negatively charged phospholipids. This is indeed suggested by the higher membrane depolarization observed for chimeras containing Bax- α 5. For this reason, in the following stages of our work we focus on the Bax- α 5 active fragment, as a prototype for proof-of-concept evaluation.

A synthetic peptide corresponding to Bax residues 106-134 exhibits potent mitochondrial-poration activity

Based on the above findings, we tested whether a synthetic peptide with the sequence of helix α 5 from Bax, residues Asn¹⁰⁶ to Arg¹³⁴ (Fig. S3, panel A, inset), can induce cytochrome c release from freshly prepared mitochondria (isolated from SK-MEL-28 metastatic human melanoma cells). A 5-min exposure to 10 μ M of the Bax[106-134] peptide was sufficient to cause significant release of mitochondrial cytochrome c, and a concentration of 25 μ M completely depleted all mitochondrial cytochrome c after the same incubation time (Fig. S3A, panel A, top). For comparison, we also assayed a peptide corresponding to the BH3 domain of Bax (helix- α 2), which was found to have no effect (Fig. S3, panel A, middle). Importantly, unlike the Bax[106-134] peptide, the synthetic (KLAKLAK)₂ peptide was unable to release cytochrome c from isolated mitochondria (Fig. S3, panel A, bottom). These results demonstrate that a synthetic, native (non-optimized) peptide encompassing the helix- α 5 of Bax can on its own disrupt mitochondrial membrane permeability and induce release of cytochrome c. Such an activity is specific of this Bax-derived sequence, as it is not observed at comparable conditions by using another helical fragment of Bax with no reported poration activity (helix- α 2, i.e. Bax-BH3.). This peptide derived from the BH3 domain of Bax displayed only a weak activity, starting at 25 μ M after 30-60 min of peptide exposure, using human embryonic kidney HEK293T cells. Additionally, a similar activity is also not observed for the antimicrobial peptide (KLAKLAK)₂, showing that the sequence of the Bax[106-134] active fragment has been optimized during natural evolution for this particular function. Further support for the mitochondrial disruption capacity of Bax[106-134] was obtained by measuring peptide-induced swelling ($SD_{50} = 3.98 \pm 0.57 \mu$ M) and $\Delta\Psi$ m dissipation ($DD_{50} = 1.68 \pm 0.39 \mu$ M) (Fig. S3, panel B) on liver mitochondria, two characteristics indicative of mitochondrial membrane permeabilization. These results illustrate the particularly strong

capacity of the Bax[106-134] peptide to trigger mitochondrial membrane perforation. Moreover, they provide rationale for the development of MOM-permeabilizing peptides inspired by helix $\alpha 5$ of Bax, which may then be used to induce apoptosis in cancer cells.

Bax[106-134] fused to an octarginine cell penetrating motif induces caspase-dependent cell death

Next, we set out to investigate the effect of the Bax[106-134] peptide in cultured cells. One requirement for these experiments is the efficient delivery of the peptide, which should first cross the cell membrane to reach mitochondria and induce MOM permeabilization. In order to drive translocation across the plasma membrane, we used a modified version of the peptide with a poly-Arg sequence at the N-terminus (eight residues) connected to the natural sequence through a Gly linker (R8-Bax[106-134]). In addition, the peptide was derivatized with a fluorescent FITC label at its N-terminus to allow easy detection. A control peptide with similar design but with a scrambled version of the Bax[106-134] natural sequence was also synthesized (R8-Bax[Scr]). This scrambled version will not be amphipathic in its expected membrane-bound α -helix conformation. Dose-response analyses were undertaken, incubating HeLa cells with the peptides at different concentrations and different exposure times, monitoring cellular uptake and cell viability. Fluorescence microscopy revealed uptake of both peptides, with strong green fluorescence observed in the cytoplasm as early as 1h after exogenous administration at a concentration of 10 μ M (Fig. 4A). However, although R8-Bax[Scr] penetrated efficiently into HeLa cells, this peptide did not produced any significant cellular toxicity, as assessed by lactate dehydrogenase (LDH) release (Fig. 4B). In contrast, R8-Bax[106-134] induced cell death in a dose- and time-dependent manner with LC₅₀ ~ 15 μ M at 24h. As depicted in Fig. 4C, the R8-Bax[106-134]-induced LDH release was significantly diminished by incubation with zVAD.fmk, suggesting that cell death follows a caspase-dependent pathway. This observation was supported by Hoechst/propidium iodide double staining analysis (Fig. 4D), which confirmed that cell death was due to apoptosis. Moreover, we found that R8-Bax[106-134] induced similar levels of toxicity (analyzed by flow cytometry using Annexin-V binding) in Bax/Bak-deficient mouse embryonic fibroblasts (MEF DKO) and wild-type cells (MEF) (Fig. 5), whereas the corresponding scrambled peptide R8-Bax[Scr] had no effect. Treatment with the caspase inhibitor zVAD.fmk blunted R8-Bax[106-134]-induced cytotoxicity in both cell types. These results further confirm that the cell death observed is independent of both BAX and BAK (consistent with our previous

1 data using isolated mitochondria, (Guillemin et al.)) and is occurring via caspase-dependent
2 apoptosis. The R8-Bax[Scr] version can also be considered as a control to show that the cell
3 death induced by R8-Bax[106-134] is not linked to the presence of the R8 sequence. We
4 formally demonstrated that cytotoxicity was R8-independent by microinjecting into zebrafish
5 eggs and human melanoma SK-MEL-28 cells a 'naked' Bax[106-134] peptide (not fused to
6 any protein transduction domain) or an octa-arginine peptide (R8). Results showed that the
7 apoptotic activity of R8-Bax[106-134] was specific of the natural Bax- $\alpha 5$ sequence and not of
8 the membrane translocating poly-Arg motif (Fig. **S4** and Fig. **S5**).

10 ***Cytotoxic Bax[106-134] injected peritumorally shows antitumor activity in vivo***

12 Fluorescence data obtained using a non-invasive live animal imaging technology indicated
13 that, upon peritumoral administration, a Cy5-labeled Bax[106-134] peptide was mainly taken
14 up by the tumor tissue, which exhibited strong Cy5 fluorescence intensity even 24h after
15 injection (Fig. **S6**, panel A). Moreover, *ex vivo* fluorescence images of excised tumor tissues
16 indicated minor accumulation to adjacent normal tissue (Fig. **S6**, panel B). These fluorescence
17 data suggested that the Cy5-labeled peptide had a sustained localization within the tumor
18 micro-environment following peritumoral injection, which prompted us to investigate the
19 anti-tumor activity of Bax[106-134] using this administration mode. To test the antitumor
20 efficacy, the R8-Bax[106-134] version, or control samples (the scrambled R8-Bax[Scr]
21 peptide or buffer alone), were injected peritumorally 5 times a week for 2 weeks in mammary
22 adenocarcinoma (TS/A-pc) tumor-bearing athymic nude mice. As shown in Fig. **6**, after 2
23 weeks of peritumoral administration, the tumor volume was sharply reduced in the group
24 treated with R8-Bax[106-134], compared to the control groups. There was a statistically
25 significant decrease in tumor size, tumor doubling time and growth. Moreover, tumor size
26 reduction correlated with an increase in caspase-3 positive cells in tumor tissue extracts
27 indicating cell death (Fig. **6**, *inset*).

30 **DISCUSSION**

32 Aside from the intrinsic biotechnological potential of biodiversity, properties of molecules
33 found in Nature can be mimicked or extended to produce novel bioactive substances. In this
34 respect, the BH3-mimetic strategy represents a relevant example of the translation of

1 molecular discoveries into potential clinical applications (Yip and Reed, 2008). Membrane-
2 active peptides acting on the MOM (i.e. able to induce cytochrome c release and apoptosis)
3 represent yet another type of promising, but so far unexploited, candidates in the cancer
4 research field (Chen et al., 2001; Ellerby et al., 1999; Foillard et al., 2008; Law et al., 2006;
5 Mai et al., 2001; Marks et al., 2005; Rege et al., 2007). Such a strategy has some parallel with
6 the development of antibiotics from natural antimicrobial peptides (Marr et al., 2006), and in
7 fact the use of these latter systems as anticancer drugs has already been proposed (Ellerby et
8 al., 1999; Mader and Hoskin, 2006; Papo and Shai, 2005). As a singular advantage, and
9 unlike the pro-apoptotic BH3-derived peptides or BH3-like compounds, mitochondrial
10 membrane disrupting peptides will be active in cancer cells that do not express Bcl-2-like
11 proteins, or in neo-angiogenic endothelial cells irrespective of the Bcl-2 family status.
12 Additionally, compared to other membranolytic peptides of different sources, active
13 fragments designed from pore forming Bcl-2 proteins can be considered to be naturally
14 optimized by evolution to act on mitochondrial membranes (Guillemin et al.). Here, we have
15 shown that a peptide (Bax[106-134]) derived from the pore-forming domain of pro-apoptotic
16 Bax can cause mitochondrial damage and caspase-dependent apoptosis. This peptide appears
17 to carry sufficient structural information to insert into the MOM, causing $\Delta\Psi_m$ loss,
18 membrane disruption and cytochrome c release. Moreover, it produced (when fused to a
19 polyarginine transduction motif) potent anticancer activity after peritumoral injection in
20 tumor-bearing mice presumably by inducing tumor cell apoptosis.

21
22 The molecular mechanism of pore formation and the structural properties of different peptide
23 versions encompassing the sequence of helix $\alpha 5$ from Bax (which were very similar to
24 Bax[106-134]) have been studied in several recent papers (Garcia-Saez et al., 2007; Garcia-
25 Saez et al., 2005; Garcia-Saez et al., 2006; Guillemin et al.; Qian et al., 2008). These different
26 versions of the $\alpha 5$ fragment of Bax exhibited strong α -helical propensity in model lipid
27 membranes and were shown to form lipidic pores of toroidal structure (Garcia-Saez et al.,
28 2005; Qian et al., 2008). A similar mechanism of pore formation has been proposed for
29 cationic α -helical antimicrobial peptides like magainin (Ludtke et al., 1996). Although Bax
30 has also been proposed to form pores of the proteo-lipidic toroidal type (Terrones et al.,
31 2004), its mechanism of action is still largely unknown. A major difference between the
32 activity of complete Bax, compared to that of Bax fragments, towards mitochondrial
33 membranes is the existence of upstream (yet unclear) regulatory events, leading to Bax
34 activation via structural reorganization and membrane binding. Additionally, in the active

membrane-bound state, the Bax protein surely forms a larger and more complex oligomer and pore than Bax-derived peptides. Nevertheless, our results are consistent with the main findings reported in the literature for Bax action. First, the GFP fusion to complete Bax shows no specific localization to mitochondria (Fig. 2), weak disrupting activity towards this organelle (Fig. 3 and S2) and weak apoptosis induction (Fig. 1 and S1). This result is in accordance with the notion that monomeric Bax has to be activated by tBid previous to its targeting, oligomerization and poration of the MOM (Billen et al., 2008; Lovell et al., 2008; Terrones et al., 2004). In contrast, Bax fragments display a clearly different behaviour. Fusions of GFP with Bax fragments containing $\alpha 5$, $\alpha 6$ and/or $\alpha 9$, either alone or in the $\alpha 5$ - $\alpha 6$ or $\alpha 5$ - $\alpha 9$ constructions, all localize specifically and intrinsically to mitochondria (Fig. 2). In contrast, the fusions containing only the $\alpha 5$ and $\alpha 6$ fragments as well as the $\alpha 5$ - $\alpha 6$ hairpin miniature exhibit a high mitochondria-disrupting activity (Fig. 3 and S2), which, in turn, correlates with strong cell death induction (Fig. 1 and S1). These latter and most remarkable observations are consistent with the existence in Bax of several independent mitochondrial targeting sequences, located in helices $\alpha 5$, $\alpha 6$ and $\alpha 9$ (George et al., 2007; George et al.; Schinzel et al., 2004; Valentijn et al., 2008). Thus, our results show that the naked versions of these fragments have a natural tendency for specific binding to the MOM, and in the cases of $\alpha 5$ and $\alpha 6$ for high membrane poration activity, with no need for complex structural reorganization, as they are intrinsically active. Within the context of larger domains, intra- and inter-molecular interactions between different helices of Bax (George et al., 2007; George et al.; Suzuki et al., 2000) may impair their interaction with the membrane. This phenomenon, which is at the origin of the regulation of the complete Bax protein, might also be among the reasons why the GFP-Bax $\alpha 5$ - $\alpha 9$ construct was not as potent as Bax $\alpha 5$, - $\alpha 6$ and - $\alpha 5\alpha 6$ in causing cell death (Fig. 1 and S1).

In conclusion, although Bax-derived fragments can obviously not mimic the elaborate behaviour of the full length protein, considering fundamental aspects of their membrane activity, these peptides represent in practice minimal versions of Bax, evolutionary-designed to target, bind and porate mitochondria. Thus, Bax[106-134] shows a specificity and efficacy for MOM disruption clearly overcoming that of the cationic peptide (KLAKLAK)₂, in agreement with the low potency previously reported for this molecule (Borgne-Sanchez et al., 2007; Ellerby et al., 1999). Additionally, the lack of regulatory capacity in minimal peptide versions with respect to full-length Bax renders these molecules intrinsically and

1 autonomously active, which may be used advantageously as a basis for antitumor therapy.
2 Thus, we propose to exploit membrane-active segments from natural Bcl-2-like templates
3 (such as helices $\alpha 5/6$ of Bax) to develop a new generation of mitochondria-targeted cytotoxic
4 agents (named ‘poropeptides’). To be applicable in cancer therapy, poropeptides should
5 eliminate tumor cells without being harmful to normal cells. Indeed, although such
6 biologically active peptides can be developed into drugs, design of suitable delivery systems
7 for site-specific targeting to tumors remains the most challenging task. Future work will
8 therefore focus on endowing therapeutic poropeptides with the ability to reach tumor cells and
9 leave normal cells unharmed.

12 MATERIAL AND METHODS

14 Peptides

15 Bax[106-134], Bax-BH3, FITC-R8-Bax[106-134], FITC-R8-Bax[Scr] and R8 peptides were
16 purchased from GeneCust EUROPE at a 2 or 5 mg scale and purified to >95% by HPLC. R8-
17 Bax[106-134] and R8-Bax[Scr] were prepared by solid-phase synthesis as reported (Garcia-
18 Saez et al., 2005) in an Applied Biosystems ABI 433A Peptide synthesizer (Foster City, CA,
19 USA) using Fmoc chemistry and Tentagel S-RAM resin (Rapp Polymere, Tübingen,
20 Germany; 0.24 mEq/g substitution) as a solid support. Peptides were purified using a C18
21 semi-preparative reversed-phase column (Merck, Darmstadt, Germany) by HPLC, to a >95%
22 purity, and their identity was confirmed by Mass Spectrometry. Peptide concentrations were
23 determined from UV spectra using a Jasco spectrophotometer (Jasco, Tokyo, Japan). The
24 Cyanine5-Bax[106-134] peptide was synthesized using solid-phase peptide synthesis (SPPS),
25 purified by HPLC and characterized by ESMS at the chemistry platform ‘NanoBio campus’
26 (Grenoble, France). R8 (arginine-8) peptides had an amide group at their C-terminus. The
27 amino acid sequences of the peptides are shown in **Table I**.

29 Antibodies

30 Primary antibodies were as follows: mouse monoclonal Anti-mitochondrial-HSP70 (Abcam),
31 anti-GFP mouse monoclonal antibody (Roche), anti-cleaved caspase-3 rabbit polyclonal
32 antibody (Cell Signaling Technology), anti-cleaved PARP (Abcam), anti- α -tubulin antibody
33 (Santa Cruz Biotechnologies) and anti-cytochrome c antibody. HRP-conjugated goat anti-

mouse and goat anti-rabbit secondary antibodies (Roche) were used as secondary antibodies. Western Blot analysis was performed according to standard procedures.

Cell culture

SK-MEL-28 human melanoma cells and HeLa cells were cultured at 37°C and 5% CO₂ in MEM supplemented with 10% FBS, 1% penicillin/streptomycin and 1% of non-essential amino acids. HT1080 cells, HEK293T cells, MEF and MEF-DKO mouse embryonic fibroblasts cells were cultured in DMEM supplemented with 10% FBS and 1% Penicillin/Streptomycin. For transient transfection, cells were plated at a density of 10⁵ cells per 35mm plate) and allowed to grow for 24h before transfection with plasmids using the Lipofectamine2000 (Invitrogen) according to the manufacturer's recommendation. For each transfection 3 µg plasmid DNA was used. Caspase inhibitor zVAD.fmk was purchased from Bachem. TS/A-pc mice mammary carcinoma cells were cultured in RPMI 1640 supplemented with 1% glutamine, 10% FBS, 50 units/ml penicillin, and 50 µg/ml streptomycin at 37°C in a humidified 95% air / 5% CO₂ atmosphere. These cells are integrin αvβ3-positive (Klepfish et al., 1993; Sancey et al., 2007).

Molecular cloning

The oligonucleotides (Sigma-Proligo) that were used to prepare the different constructions are indicated in **Table S1**. All the constructions were subcloned into pGEM-T Easy (Promega) and then subsequently subcloned into XhoI and KpnI sites of pEGFP-C1. The sequence of all constructs was verified by automated sequencing (GEXbyWeb).

Measurement of cell death and viability

Hoechst/PI labeling of cells to detect apoptotic and necrotic cell death were performed as described previously (Dive et al., 1992). Hoechst 33342 and PI were from Molecular Probes (Invitrogen). LDH cytotoxicity assay was performed according to the manufacturer's protocol (LDH Cytotoxicity Assay Kit II, Biovision Research Products, CA); the colorimetric assay quantifies LDH activity released from the cytosol of damaged cells into the supernatant and thus serves to quantify cell death. Cytotoxicity assays were performed in triplicates in each of two or three independent experiments. Cell death was quantified by Annexin-V-Cy3 (BioVision Inc.) staining according to manufacturer's protocols, followed by flow cytometric analysis using a FACScan (Becton Dickinson). Data were processed using CellQuest Pro (version 4.0) software.

Mitochondrial assays

In vitro assessment of mitochondrial parameters (swelling and $\Delta\Psi_m$ loss) was performed on liver mitochondria as previously described (Jacotot et al., 2006). Mitochondrial membrane potential was measured using the fluorescent dye Mito-Tracker Red (Molecular Probes), which emits fluorescence in cells with an intact $\Delta\Psi_m$. Transfected cells were incubated with Mito-Tracker Red (50 nM for 2h min at 37 °C). Cells were observed under a fluorescence microscope and the percentage of green cells that were Mito-Tracker positive was determined (~100 cells in each experiment). For flow cytometry analysis, HT1080 cells were washed twice with serum-free medium and then resuspended in PBS. Flow cytometric analysis was performed using a LSR II (Becton Dickinson) and data were processed using FACSDiva (version 6.1.2) software.

Confocal microscopy analysis

Cells were fixed in 4% paraformaldehyde, permeabilized in 0.1% Triton X-100 for 3 minutes, and treated with TO-PRO-3 iodide (final 2 μ M, Molecular Probes) before mounting in a drop of anti-bleaching medium. Confocal analysis was performed on a Zeiss confocal microscope (LSM510) (LePecq, France) with a plan apochromat 63 \times 1.4 oil immersion objective. Images were collected under identical non-saturated conditions after multiple scans (~ 8 sections per cell).

***In vivo* experiments**

All the animal experiments were performed in agreement with the EEC guidelines and the “Principles of laboratory animal care” (NIH publication 14N°86-23 revised 1985). The experimental protocol was submitted to ethical evaluation and the experiment received the accreditation number #323. The investigator possesses the authorization number #38-09-22 (Sancey L.)

Tumor regression assays

Mouse mammary TS/A-pc cells were harvested from culture, and 10⁶ cells in sterile PBS were injected subcutaneously into the flank of thirty female Balb/c mice. Three days after injection, mice were randomized into three experimental groups (9 mice/group). Group 1 (control mice) received vehicle (PBS), group 2 received Bax[106-134], and group 3 received

1 Bax-Scr.

2 One hundred μg peptide/mouse (100 μl /mouse) was administered peritumorally, 5 times a
3 week for 2 weeks. Tumor growth was assessed by measuring tumor size in two dimensions
4 using a Vernier caliper each day after tumor size reaches 10 mm^3 or larger (from day 10).
5 Tumor volume was calculated as follows: $(\pi/6) \times a \times b^2$, where a and b are the largest and
6 smallest diameters, respectively (Kjonnixsen et al., 1989; Olea et al., 1992). Results are
7 expressed as mean \pm S.E.M. None of the mice had developed necrotic tumors or tumors ≥ 1.5
8 cm in diameter. On day 14, all mice were sacrificed to prevent lung metastasis, especially in
9 groups 1 and 3. The tumor doubling time (TDT) was calculated as $(T_d' - T_d) \ln 2 / (\ln(V_d' - V_d))$,
10 where T is time at days d and d' and V is the corresponding tumor volume.

12 Statistical analysis

13 For the *in vivo* studies, results were analyzed by *t*-test for unmatched groups (Statview
14 software, SAS Institute, Inc.): *p* values < 0.05 were considered statistically significant.

17 ACKNOWLEDGEMENTS

19 We wish to thank Julien Thibaut, Agnès Cibiél, Clara Locher, Jonathan Lopez and Sonia
20 Schott for help during the initial stages of this work, Gustavo Fuertes (Universidad de
21 Valencia, España) and Eric Diesis (IBCP) for the provision of peptides, Aurélie Cornut for
22 guidance in cloning, Annie Borgne-Sanchez at Mitologics, Marie-Hélène Ratinaud and
23 Nathalie Bonnefoy-Bérard for discussion. The MitoRed plasmid was a kind gift from Dr.
24 Dong. JGV is recipient of doctoral fellowship from La Région Rhône-Alpes. LS is granted by
25 ANR PNANO. We are indebted to Jean Paufigue, Brigitte Closs, Sylvie Bordes and Sandrine
26 Magnetto for their constant support and for their continuous interest in this work. This work
27 was supported by grants from the Silab-Jean Paufigue Corporate Foundation (France), La
28 Ligue Contre le Cancer (Comités de la Drôme et du Rhône), the Spanish MEC (BFU2007-
29 67097) and a collaborative French/Spanish project (EGIDE PHC PICASSO 17092SM; MEC,
30 HF2007-0090).

33 CONFLICT OF INTEREST

34 The authors declare that they have no conflict of interest.

REFERENCES

- Adams, J. M. and Cory, S. (2007). The Bcl-2 apoptotic switch in cancer development and therapy. *Oncogene* **26**, 1324-37.
- Annis, M. G., Soucie, E. L., Dlugosz, P. J., Cruz-Aguado, J. A., Penn, L. Z., Leber, B. and Andrews, D. W. (2005). Bax forms multispinning monomers that oligomerize to permeabilize membranes during apoptosis. *Embo J* **24**, 2096-103.
- Aouacheria, A., Cibiel, A., Guillemin, Y., Gillet, G. and Lalle, P. (2007). Modulating mitochondria-mediated apoptotic cell death through targeting of Bcl-2 family proteins. *Recent Pat DNA Gene Seq* **1**, 43-61.
- Bellot, G., Cartron, P. F., Er, E., Oliver, L., Juin, P., Armstrong, L. C., Bornstein, P., Mihara, K., Manon, S. and Vallette, F. M. (2007). TOM22, a core component of the mitochondria outer membrane protein translocation pore, is a mitochondrial receptor for the proapoptotic protein Bax. *Cell Death Differ* **14**, 785-94.
- Billen, L. P., Kokoski, C. L., Lovell, J. F., Leber, B. and Andrews, D. W. (2008). Bcl-XL inhibits membrane permeabilization by competing with Bax. *PLoS Biol* **6**, e147.
- Borgne-Sanchez, A., Dupont, S., Langonne, A., Baux, L., Lecoeur, H., Chauvier, D., Lassalle, M., Deas, O., Briere, J. J., Brabant, M. et al. (2007). Targeted Vpr-derived peptides reach mitochondria to induce apoptosis of alphaVbeta3-expressing endothelial cells. *Cell Death Differ* **14**, 422-35.
- Cartron, P. F., Arokium, H., Oliver, L., Meflah, K., Manon, S. and Vallette, F. M. (2005). Distinct domains control the addressing and the insertion of Bax into mitochondria. *J Biol Chem* **280**, 10587-98.
- Chen, Y., Xu, X., Hong, S., Chen, J., Liu, N., Underhill, C. B., Creswell, K. and Zhang, L. (2001). RGD-Tachyplesin inhibits tumor growth. *Cancer Res* **61**, 2434-8.
- Dive, C., Gregory, C. D., Phipps, D. J., Evans, D. L., Milner, A. E. and Wyllie, A. H. (1992). Analysis and discrimination of necrosis and apoptosis (programmed cell death) by multiparameter flow cytometry. *Biochim Biophys Acta* **1133**, 275-85.
- Ellerby, H. M., Arap, W., Ellerby, L. M., Kain, R., Andrusiak, R., Rio, G. D., Krajewski, S., Lombardo, C. R., Rao, R., Ruoslahti, E. et al. (1999). Anti-cancer activity of targeted pro-apoptotic peptides. *Nat Med* **5**, 1032-8.
- Foillard, S., Jin, Z. H., Garanger, E., Boturyn, D., Favrot, M. C., Coll, J. L. and Dumy, P. (2008). Synthesis and biological characterisation of targeted pro-apoptotic peptide. *Chembiochem* **9**, 2326-32.
- Foillard, S., Sancey, L., Coll, J. L., Boturyn, D. and Dumy, P. (2009). Targeted delivery of activatable fluorescent pro-apoptotic peptide into live cells. *Org Biomol Chem* **7**, 221-4.
- Fuertes, G., Giménez, D., Esteban-Martin, S., Garcia-Saez, A. J., Sanchez, O. and Salgado, J. (2010). Role of Membrane Lipids for the Activity of Pore Forming Peptides and Proteins. In *Proteins: Membrane Binding and Pore Formation*, (ed. L. Bioscience). Austin, TX: Landes Bioscience.
- Garcia-Saez, A. J., Chiantia, S., Salgado, J. and Schwille, P. (2007). Pore formation by a Bax-derived peptide: effect on the line tension of the membrane probed by AFM. *Biophys J* **93**, 103-12.

1 **Garcia-Saez, A. J., Coraiola, M., Dalla Serra, M., Mingarro, I., Menestrina, G.**
2 **and Salgado, J.** (2005). Peptides derived from apoptotic Bax and Bid reproduce the poration
3 activity of the parent full-length proteins. *Biophys J* **88**, 3976-90.

4 **Garcia-Saez, A. J., Coraiola, M., Serra, M. D., Mingarro, I., Muller, P. and**
5 **Salgado, J.** (2006). Peptides corresponding to helices 5 and 6 of Bax can independently form
6 large lipid pores. *Febs J* **273**, 971-81.

7 **Garcia-Saez, A. J., Mingarro, I., Perez-Paya, E. and Salgado, J.** (2004).
8 Membrane-insertion fragments of Bcl-xL, Bax, and Bid. *Biochemistry* **43**, 10930-43.

9 **George, N. M., Evans, J. J. and Luo, X.** (2007). A three-helix homo-oligomerization
10 domain containing BH3 and BH1 is responsible for the apoptotic activity of Bax. *Genes Dev*
11 **21**, 1937-48.

12 **George, N. M., Targy, N., Evans, J. J., Zhang, L. and Luo, X.** Bax contains two
13 functional mitochondrial targeting sequences and translocates to mitochondria in a
14 conformational change- and homo-oligomerization-driven process. *J Biol Chem* **285**, 1384-
15 92.

16 **Guillemin, Y., Lopez, J., Gimenez, D., Fuertes, G., Valero, J. G., Blum, L.,**
17 **Gonzalo, P., Salgado, J., Girard-Egrot, A. and Aouacheria, A.** Active Fragments from
18 Pro- and Antiapoptotic BCL-2 Proteins Have Distinct Membrane Behavior Reflecting Their
19 Functional Divergence. *PLoS One* **5**, e9066.

20 **Heimlich, G., McKinnon, A. D., Bernardo, K., Brdiczka, D., Reed, J. C., Kain, R.,**
21 **Kronke, M. and Jurgensmeier, J. M.** (2004). Bax-induced cytochrome c release from
22 mitochondria depends on alpha-helices-5 and -6. *Biochem J* **378**, 247-55.

23 **Jacotot, E., Deniaud, A., Borgne-Sanchez, A., Touat, Z., Briand, J. P., Le Bras,**
24 **M. and Brenner, C.** (2006). Therapeutic peptides: Targeting the mitochondrion to modulate
25 apoptosis. *Biochim Biophys Acta* **1757**, 1312-23.

26 **Jansson, A. and Sun, X. F.** (2002). Bax expression decreases significantly from
27 primary tumor to metastasis in colorectal cancer. *J Clin Oncol* **20**, 811-6.

28 **Jin, Z. H., Josserand, V., Razkin, J., Garanger, E., Boturyn, D., Favrot, M. C.,**
29 **Dumy, P. and Coll, J. L.** (2006). Noninvasive optical imaging of ovarian metastases using
30 Cy5-labeled RAFT-c(-RGDFK)-4. *Mol Imaging* **5**, 188-97.

31 **Kjonnixsen, I., Storeng, R., Pihl, A., McLemore, T. L. and Fodstad, O.** (1989). A
32 human tumor lung metastasis model in athymic nude rats. *Cancer Res* **49**, 5148-52.

33 **Klepfish, A., Greco, M. A. and Karparkin, S.** (1993). Thrombin stimulates
34 melanoma tumor-cell binding to endothelial cells and subendothelial matrix. *Int J Cancer* **53**,
35 978-82.

36 **Kolluri, S. K., Zhu, X., Zhou, X., Lin, B., Chen, Y., Sun, K., Tian, X., Town, J.,**
37 **Cao, X., Lin, F. et al.** (2008). A short Nur77-derived peptide converts Bcl-2 from a protector
38 to a killer. *Cancer Cell* **14**, 285-98.

39 **Law, B., Quinti, L., Choi, Y., Weissleder, R. and Tung, C. H.** (2006). A
40 mitochondrial targeted fusion peptide exhibits remarkable cytotoxicity. *Mol Cancer Ther* **5**,
41 1944-9.

42 **Lovell, J. F., Billen, L. P., Bindner, S., Shamas-Din, A., Fradin, C., Leber, B. and**
43 **Andrews, D. W.** (2008). Membrane binding by tBid initiates an ordered series of events
44 culminating in membrane permeabilization by Bax. *Cell* **135**, 1074-84.

45 **Ludtke, S. J., He, K., Heller, W. T., Harroun, T. A., Yang, L. and Huang, H. W.**
46 (1996). Membrane pores induced by magainin. *Biochemistry* **35**, 13723-8.

47 **Mader, J. S. and Hoskin, D. W.** (2006). Cationic antimicrobial peptides as novel
48 cytotoxic agents for cancer treatment. *Expert Opin Investig Drugs* **15**, 933-46.

49 **Mai, J. C., Mi, Z., Kim, S. H., Ng, B. and Robbins, P. D.** (2001). A proapoptotic
50 peptide for the treatment of solid tumors. *Cancer Res* **61**, 7709-12.

1 **Marks, A. J., Cooper, M. S., Anderson, R. J., Orchard, K. H., Hale, G., North, J.**
2 **M., Ganeshaguru, K., Steele, A. J., Mehta, A. B., Lowdell, M. W. et al.** (2005). Selective
3 apoptotic killing of malignant hemopoietic cells by antibody-targeted delivery of an
4 amphipathic peptide. *Cancer Res* **65**, 2373-7.

5 **Marr, A. K., Gooderham, W. J. and Hancock, R. E.** (2006). Antibacterial peptides
6 for therapeutic use: obstacles and realistic outlook. *Curr Opin Pharmacol* **6**, 468-72.

7 **Olea, N., Villalobos, M., Ruiz de Almodovar, J. M. and Pedraza, V.** (1992). MCF-
8 7 breast cancer cells grown as multicellular spheroids in vitro: effect of 17 beta-estradiol. *Int J*
9 *Cancer* **50**, 112-7.

10 **Oltersdorf, T., Elmore, S. W., Shoemaker, A. R., Armstrong, R. C., Augeri, D. J.,**
11 **Belli, B. A., Bruncko, M., Deckwerth, T. L., Dinges, J., Hajduk, P. J. et al.** (2005). An
12 inhibitor of Bcl-2 family proteins induces regression of solid tumours. *Nature* **435**, 677-81.

13 **Ouyang, H., Furukawa, T., Abe, T., Kato, Y. and Horii, A.** (1998). The BAX gene,
14 the promoter of apoptosis, is mutated in genetically unstable cancers of the colorectum,
15 stomach, and endometrium. *Clin Cancer Res* **4**, 1071-4.

16 **Papo, N., Seger, D., Makovitzki, A., Kalchenko, V., Eshhar, Z., Degani, H. and**
17 **Shai, Y.** (2006). Inhibition of tumor growth and elimination of multiple metastases in human
18 prostate and breast xenografts by systemic inoculation of a host defense-like lytic peptide.
19 *Cancer Res* **66**, 5371-8.

20 **Papo, N. and Shai, Y.** (2005). Host defense peptides as new weapons in cancer
21 treatment. *Cell Mol Life Sci* **62**, 784-90.

22 **Qian, S., Wang, W., Yang, L. and Huang, H. W.** (2008). Structure of
23 transmembrane pore induced by Bax-derived peptide: evidence for lipidic pores. *Proc Natl*
24 *Acad Sci U S A* **105**, 17379-83.

25 **Rege, K., Patel, S. J., Megeed, Z. and Yarmush, M. L.** (2007). Amphipathic
26 peptide-based fusion peptides and immunoconjugates for the targeted ablation of prostate
27 cancer cells. *Cancer Res* **67**, 6368-75.

28 **Sancey, L., Ardisson, V., Riou, L. M., Ahmadi, M., Marti-Batlle, D., Boturyn, D.,**
29 **Dumy, P., Fagret, D., Ghezzi, C. and Vuillez, J. P.** (2007). In vivo imaging of tumour
30 angiogenesis in mice with the alpha(v)beta (3) integrin-targeted tracer (99m)Tc-RAFT-RGD.
31 *Eur J Nucl Med Mol Imaging* **34**, 2037-47.

32 **Schinzl, A., Kaufmann, T., Schuler, M., Martinalbo, J., Grubb, D. and Borner,**
33 **C.** (2004). Conformational control of Bax localization and apoptotic activity by Pro168. *J*
34 *Cell Biol* **164**, 1021-32.

35 **Shiraishi, T. and Nielsen, P. E.** (2006). Enhanced delivery of cell-penetrating
36 peptide-peptide nucleic acid conjugates by endosomal disruption. *Nat Protoc* **1**, 633-6.

37 **Suzuki, M., Youle, R. J. and Tjandra, N.** (2000). Structure of Bax: coregulation of
38 dimer formation and intracellular localization. *Cell* **103**, 645-54.

39 **Terrones, O., Antonsson, B., Yamaguchi, H., Wang, H. G., Liu, J., Lee, R. M.,**
40 **Herrmann, A. and Basanez, G.** (2004). Lipidic pore formation by the concerted action of
41 proapoptotic BAX and tBID. *J Biol Chem* **279**, 30081-91.

42 **Valentijn, A. J., Upton, J. P., Bates, N. and Gilmore, A. P.** (2008). Bax targeting to
43 mitochondria occurs via both tail anchor-dependent and -independent mechanisms. *Cell*
44 *Death Differ* **15**, 1243-54.

45 **Yip, K. W. and Reed, J. C.** (2008). Bcl-2 family proteins and cancer. *Oncogene* **27**,
46 6398-406.

47 **Youle, R. J. and Strasser, A.** (2008). The BCL-2 protein family: opposing activities
48 that mediate cell death. *Nat Rev Mol Cell Biol* **9**, 47-59.

1 **Zong, W. X., Lindsten, T., Ross, A. J., MacGregor, G. R. and Thompson, C. B.**
2 (2001). BH3-only proteins that bind pro-survival Bcl-2 family members fail to induce
3 apoptosis in the absence of Bax and Bak. *Genes Dev* **15**, 1481-6.
4
5

CONFIDENTIAL

FIGURE LEGENDS

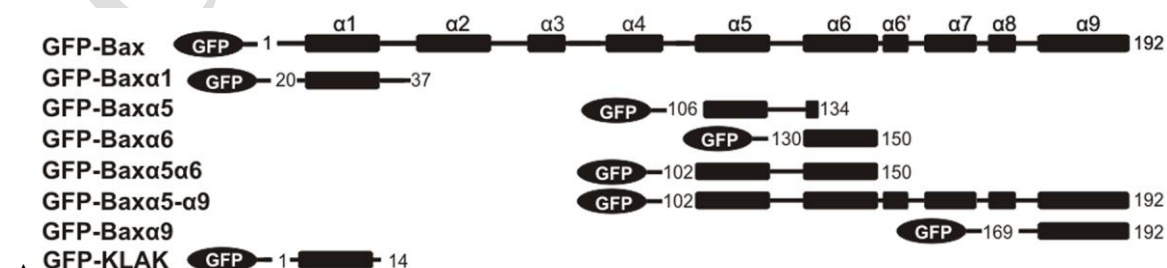
Figure 1. Ectopic overexpression of GFP-tagged Bax- α 5/ α 6 fragments induces cell death.

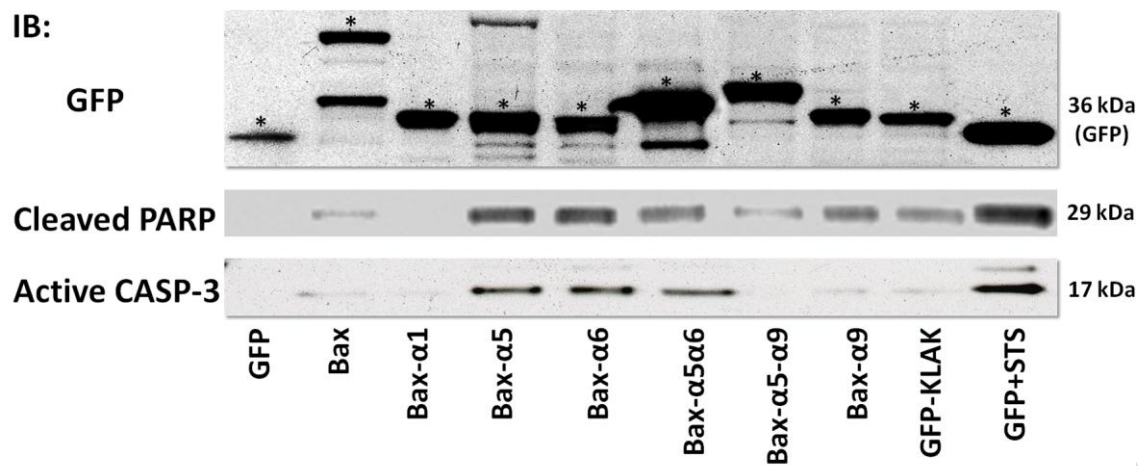
(A) Chimeric GFP proteins used in this study. GFP-tagged constructs encoding GFP alone, or fusions of GFP with full-length Bax, Bax- α 1, Bax- α 5, Bax- α 6, Bax- α 5 α 6, Bax- α 5- α 9 and Bax- α 9 are represented. The α -helical topology of Bax in solution was retrieved from (Suzuki et al., 2000). Because the structure of the membrane-bound form of Bax is unknown, we designed peptide versions that extend a few residues beyond the α -helical regions determined for the structure in aqueous buffer.

(B) Expression and analysis of the various GFP-tagged proteins in mammalian cells. Western Blot analyses on transiently transfected HT1080 cells (24h post-transfection). Proteins were separated by SDS-PAGE followed by immunoblot with anti-GFP antibody (upper panel). Asterisks indicate the various GFP fusions depicted in (A). The expected sizes are 27, 48, 29, 30.2, 33.2, 37.2, 29.7 and 28.6 kDa respectively. Analysis of caspase-3 activation (low panel, the cleaved 17kDa product indicates activated caspase-3) and PARP cleavage (middle panel, the generated 29kDa PARP fragment is shown). Similar results were obtained using MEF-DKO (not shown).

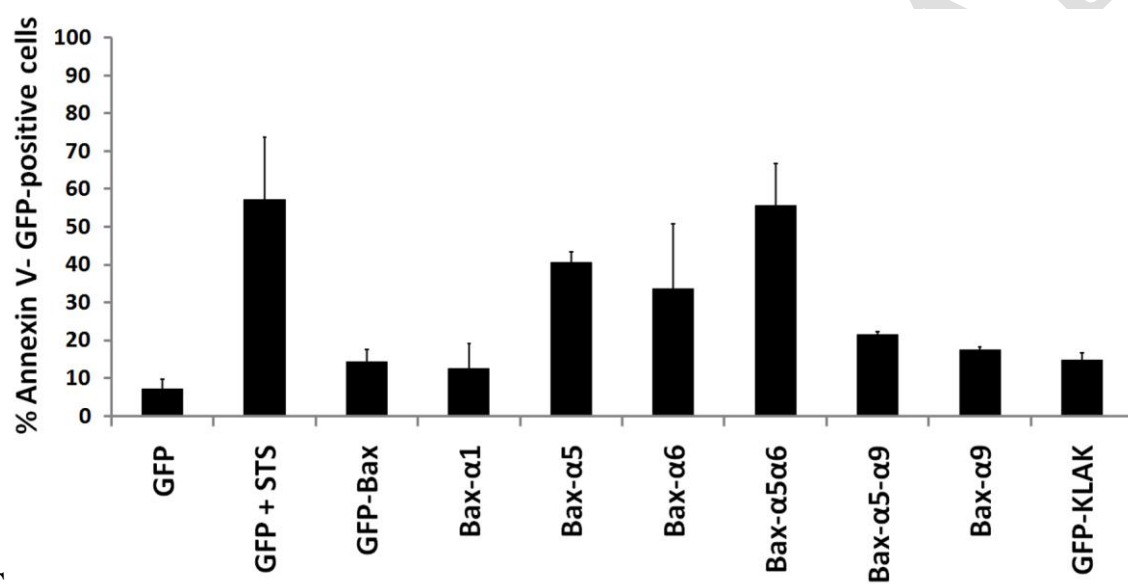
(C) FACS assays of Annexin V staining in HT1080 cells. Transfected cells were stained for phosphatidylserine exposure using Cy3-conjugated Annexin V and the percentage of apoptotic GFP-expressing cells was determined by FACS. Histograms represent the percentage of GFP-expressing cells binding Annexin V (upper panel). Assays were performed in triplicate (error bars correspond to standard deviations). GFP-[KLAKLAK]₂ transfection and staurosporine (STS) treatment were included for comparison.

(D) Primary FACS histogram overlays showing Annexin-V staining of MEF and MEF-DKO cells expressing GFP or GFP-Bax- α 5 and respectively treated with staurosporine (STS) or left untreated.

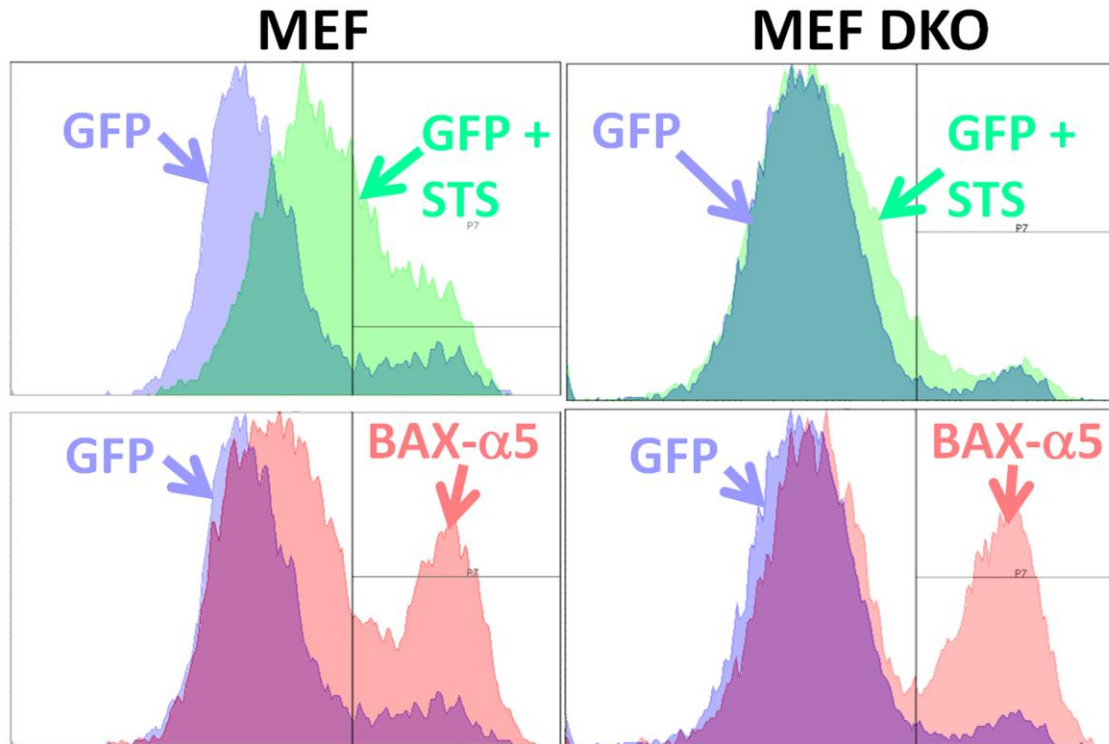




1 B



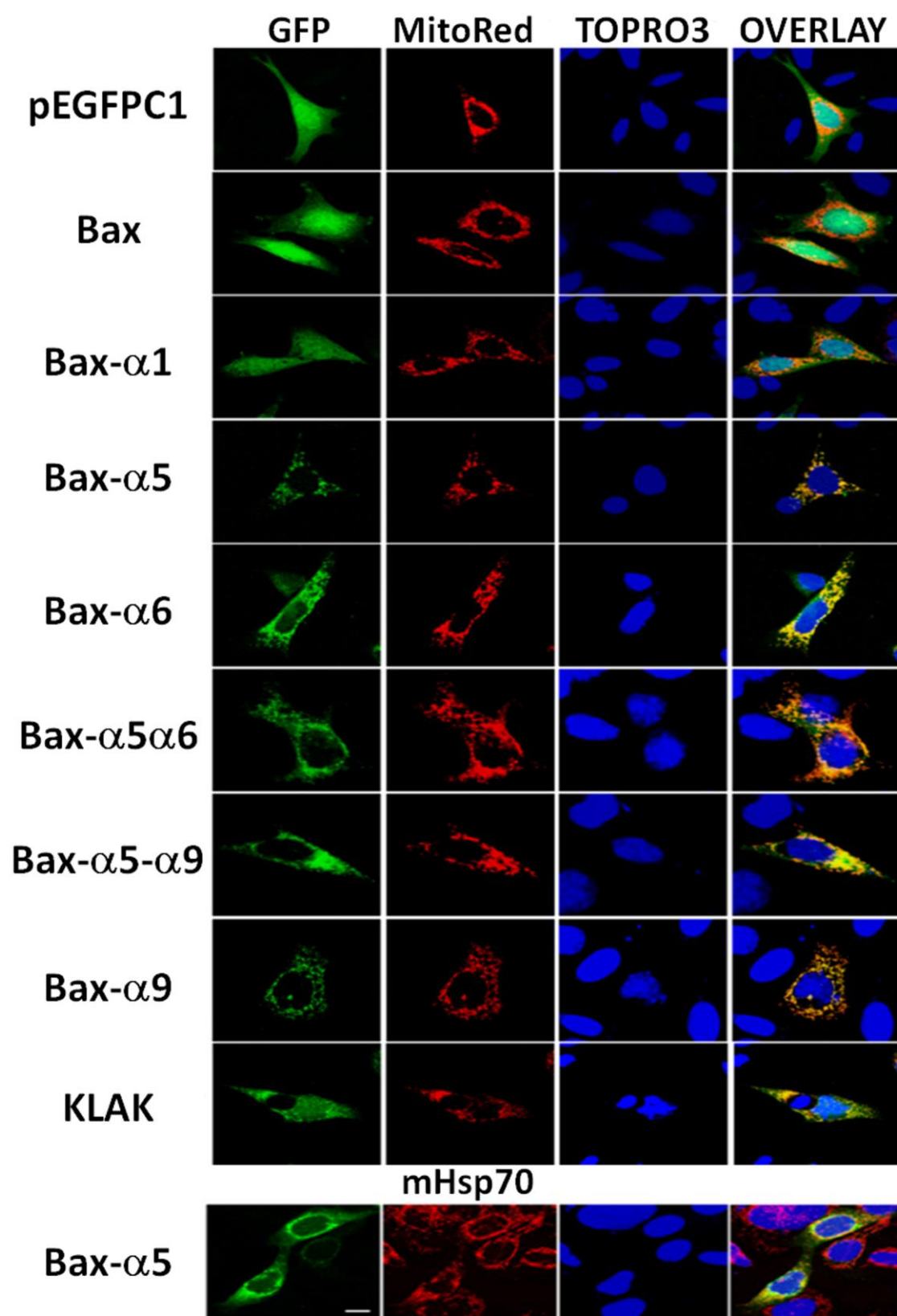
2 C



D

Figure 2. Subcellular localization of the GFP-tagged, Bax-derived (poly)peptides.

MEF-DKO cells were co-transfected with mito-DsRed plasmid (encoding DsRed2 fused to the mitochondrial targeting sequence from subunit VIII of human cytochrome c oxidase) and the GFP-tagged constructs. Subcellular distribution was analyzed by confocal microscopy 24h after transfection. Confocal images showing GFP (green) and MitoDsRed (red) fluorescence. The DNA staining dye Topro-3 (blue) was used to visualize the nuclei. In merged images, the yellow color shows the co-localization of GFP and MitoDsRed in mitochondria. Similar images were obtained using an antibody detecting mitochondrial Hsp70 (low panel). Scale bar, 10 μ m.



1
2
3
4

Figure 3. Effects of the GFP-tagged, Bax-derived (poly)peptides on mitochondrial membrane potential.

$\Delta\Psi_m$ was observed using the membrane potential sensitive probe Mitotracker-Red CMX-ROS. HT1080 cells were transfected with plasmids encoding the various GFP-tagged fusions and stained with Mitotracker-Red. GFP/Mitotracker-Red double-positive cells were counted (see Fig. S2, top panel). Data were compiled from 3 different fields (40 \times magnification). Data were compiled from 3 different fields (40 \times magnification) and represented as mean values from three independent experiments, with error bars corresponding to \pm SD. Similar results were obtained from three independent experiments. Analysis of $\Delta\Psi_m$ changes by FACS gave similar results (Fig. S2, middle and bottom panels).

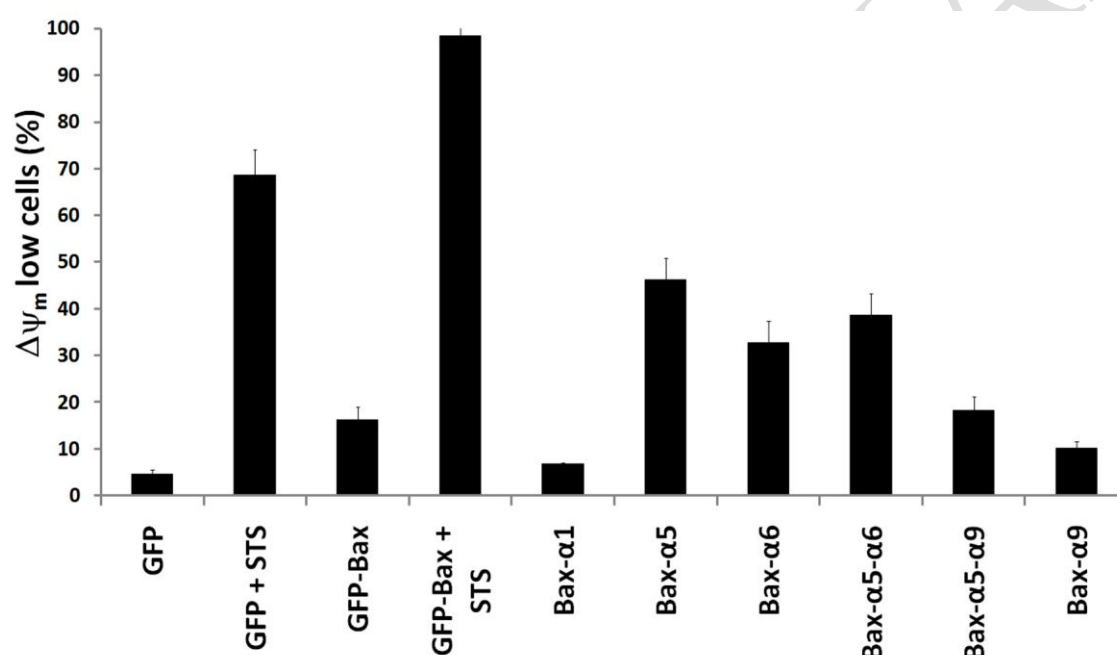


Figure 4. Synthetic peptide with the sequence of Bax[106-134] fused to an arginine octapeptide (R8-Bax[106-134]) is internalized into HeLa cells and induces caspase-dependent apoptosis.

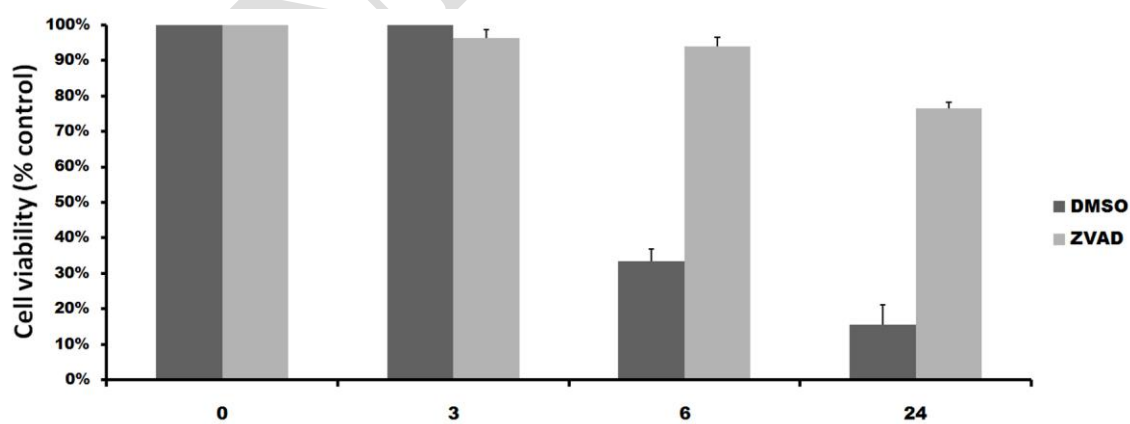
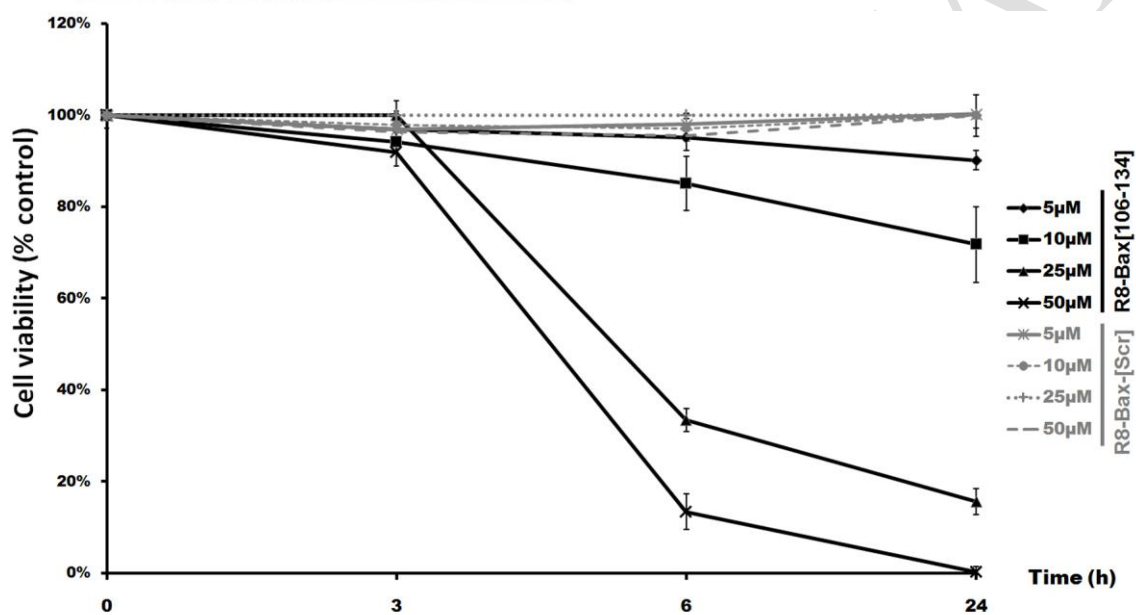
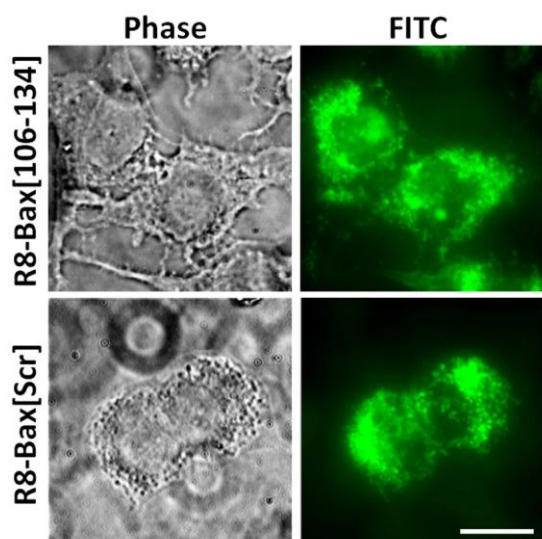
(A) HeLa cells were treated for 6h with 10 μ M R8-Bax[106-134] or with a control peptide (R8-Bax[Scr]), both conjugated to fluorescein, and observed under phase-contrast (left) or FITC epifluorescence (right, green). Cells incubated with the R8(FITC)-conjugated peptides displayed intense cytoplasmic labelling (likely associated mainly with endosomes, as shown previously (Shiraishi and Nielsen, 2006)). Scale bar, 10 μ m.

(B) Concentration- and time-dependent inhibition of cell viability of HeLa cells by R8-Bax[106-134]. HeLa cells were treated with various concentrations (5, 10, 25 and 50 μ M) of R8-Bax[106-134] or R8-Bax[Scr] peptides. Cytotoxicity was assessed by measuring lactate

1 dehydrogenase (LDH) release at 3, 6, 24h or 48h of incubation (n=4). R8-Bax[Scr] did not
2 cause any significant LDH leakage for any of the concentrations tested. Data are represented
3 as mean \pm SD.

4 (C) Caspase inhibitor zVAD.fmk reduced cell death in response to R8-Bax[106-134]. Cell
5 death was assessed by measuring LDH leakage after 24h exposure to R8-Bax[106-134] (25
6 μ M) in the absence (DMSO-treated cells) or presence of 100 μ M zVAD.fmk. Data are
7 represented as mean values \pm SD.

8 (D) Mode of cell death (apoptosis and necrosis) as revealed by Hoechst and propidium iodide
9 double staining in HeLa cells treated with the R8-Bax[106-134] peptide. Cell death was
10 quantified after 6h- or 24h treatment with 25 μ M R8-Bax[106-134]. The mode of cell death,
11 necrosis versus apoptosis, was determined by the cellular permeability to propidium iodide
12 (necrosis) and the morphology of the nuclei after staining with Hoechst 33342 (apoptosis).
13 Propidium iodide-negative cell with condensed or fragmented nuclei were counted as
14 apoptotic. Data were compiled from 3 different fields (40 \times magnification) and represented as
15 mean values from three independent experiments \pm SD.



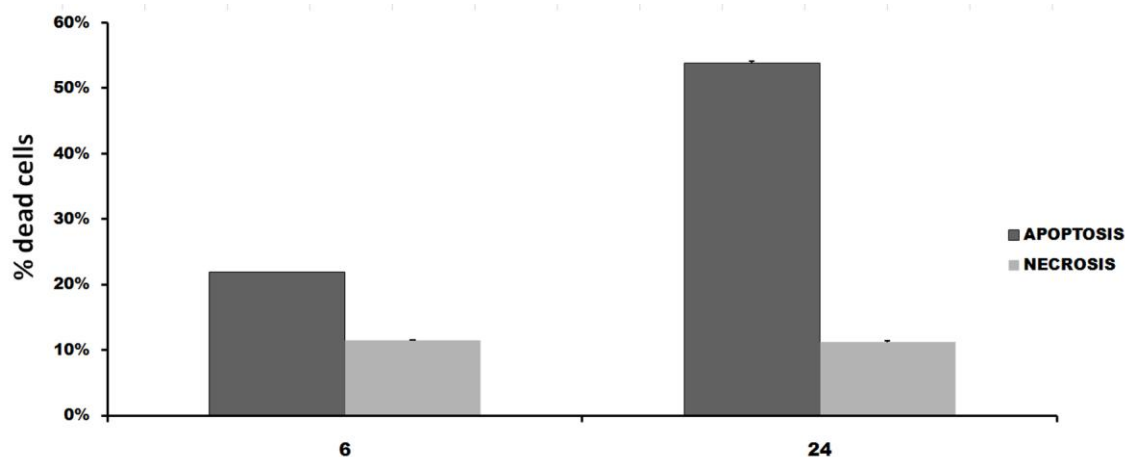


Figure 5. R8-Bax[106-134] induces Bax/Bak-independent, caspase-dependent apoptotic cell death.

Effect of treatment of Bax/Bak-deficient mouse embryonic fibroblasts (MEF DKO) or wild-type fibroblasts (MEF) with either the FITC-conjugated peptide R8-Bax[106-134] or FITC-conjugated R8-Bax[Scr], in the absence or in the presence of zVAD.fmk (100 μ M). Apoptosis was measured by flow cytometry using Annexin V-Cy3 binding at 6h and 24h. Results are presented as the percentage of apoptotic cells that had internalized the FITC-conjugated peptide (Annexin V-Cy3+/FITC+) in each condition.

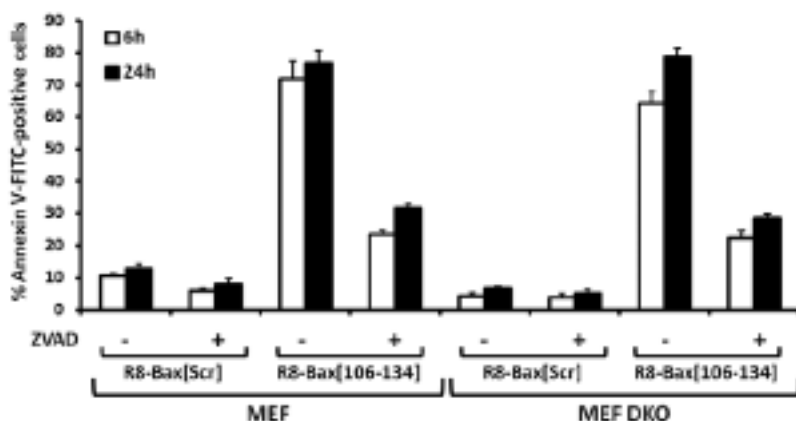
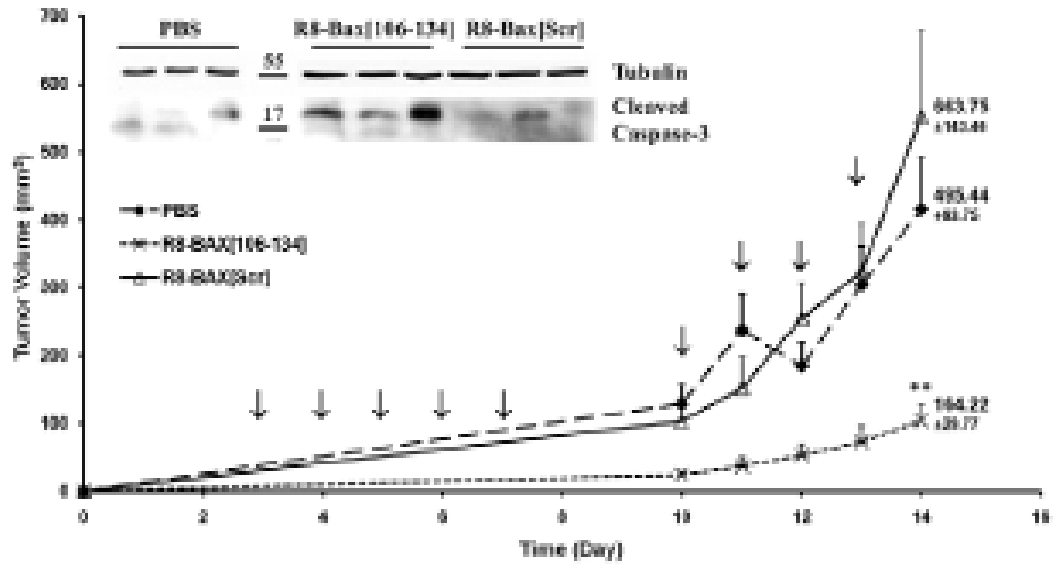


Figure 6. Antitumor effects induced by peritumoral injection of R8-Bax[106-134] in TS/A-pc mammary carcinoma xenografts.

Mouse mammary TS/A-pc carcinoma growth inhibition by Bax[106-134]. Three days after injection of tumor cells, mice (9 mice/group) received vehicle (PBS), 100 μ g of Bax[106-134], or 100 μ g of Bax-Scr peritumorally, 5 times a week for 2 weeks (arrows). Tumor volumes are indicated as mean values \pm S.E.M. The tumor doubling times (Days \pm S.E.M) were 0.493 ± 0.034 for the control group (P vs. Scramble = 0.7963, not significant), 0.692 ± 0.055 for the R8-Bax[106-134] group (P vs. control = 0.0072 ** / P vs. Scramble = 0.0063

1 **) and 0.480 ± 0.039 for the R8-Bax[Scr] group (P vs. control = 0.7963, not significant).
 2 *Inset*: protein levels of active caspase-3 in tumor extracts from each group were determined
 3 by immunoblotting. To ensure equal protein loading, membranes were also probed for
 4 tubulin. Data from triplicate samples are shown.



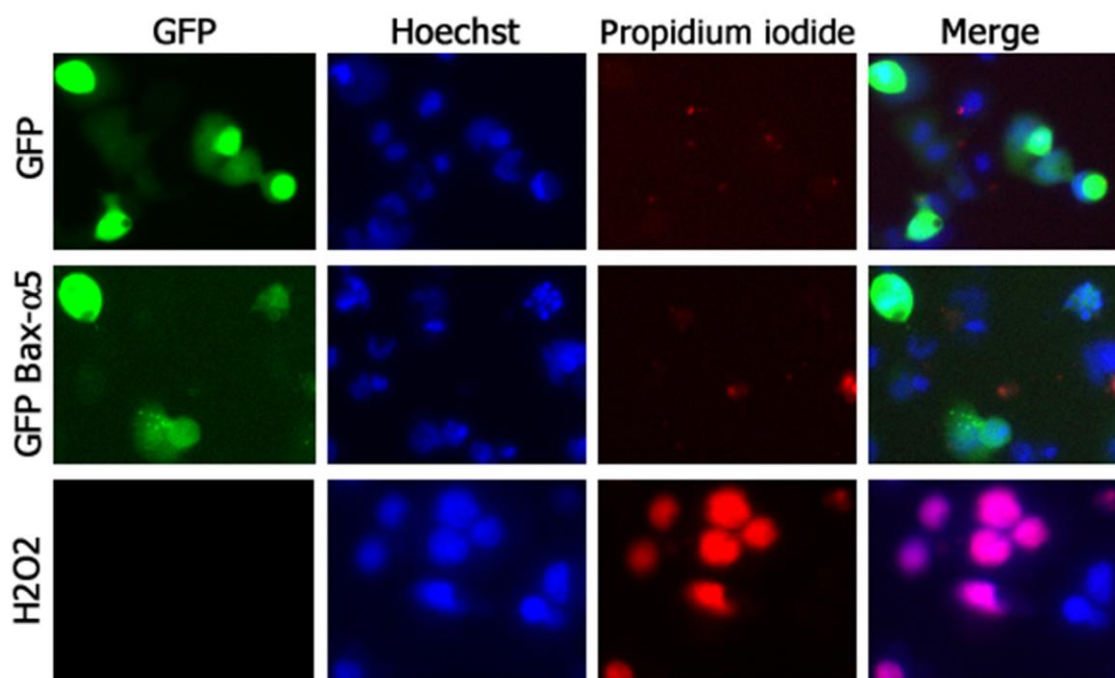
SUPPORTING INFORMATION

S1. Expression of GFP-Bax- α 5/ α 6 induces caspase-dependent and Bax/Bak-independent cell death.

Top panel: Apoptosis/Necrosis test. In this assay, apoptotic nuclei are visualized using Hoechst 33342 (blue) and necrotic or late apoptotic cells are visualized with propidium iodide (red). GFP-positive cells exhibit green fluorescence.

Middle panel: Levels of cell death (apoptosis and necrosis) in HT1080 cells expressing GFP or different GFP-tagged, Bax-derived (poly)peptides. Cells were left untreated (-) or treated with 100 μ M zVAD.fmk (+). Cell death was determined 24 hr post-transfection by analyzing GFP-positive cells (~300 cells in each experiment) under a fluorescence microscope. Data were compiled from 3 different fields (40 \times magnification). The mode of cell death, necrosis *versus* apoptosis, was determined by the cellular permeability to propidium iodide (necrosis) and the morphology of the nuclei after staining with Hoechst 33342 (apoptosis). Propidium iodide-negative cells with condensed or fragmented nuclei were counted as apoptotic. Data are represented as mean values from three independent experiments \pm SD. Experiments performed with SK-MEL-28 cells yielded similar results. GFP-[KLAKLAK]₂ transfection and staurosporine (STS) treatment were included for comparison.

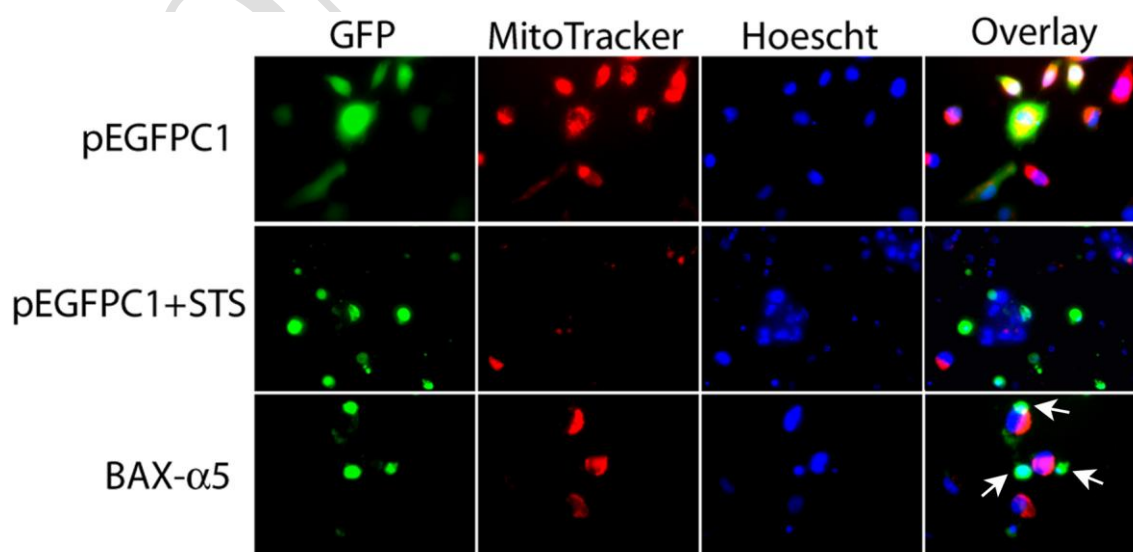
Bottom panel: Percentage of Annexin V staining in wild-type murine embryonic fibroblasts (MEF) or in Bax and Bak double knockout MEFs (DKO) transfected with control vector or with the GFP-Bax- α 5 construct. The percentage of Annexin V-binding cells was determined by FACS analysis 6h, 24, 48 and 72h after transfection using an Annexin V-Cy3 apoptosis detection kit.



S2. GFP-tagged Bax-α5/α6 fragments induce loss of mitochondrial membrane potential.

(A) Representative microscopic fields showing fluorescence of cells transfected with constructs encoding GFP (in the presence or absence of 1 μ M staurosporine) or GFP-Bax-α5. The arrows indicate GFP-Bax-α5-expressing cells that fail to exhibit MitoTracker Red staining.

(B) Flow-cytometric analysis of $\Delta\Psi_m$ estimated by MitoTracker Red intensity. HT1080 cells were transfected with control vector or with the GFP-expressing constructs and MitoTracker Red fluorescence was analyzed by flow cytometry 24h later. Results are representative of three independent experiments (up). Data are represented as mean \pm SD. A shift to the left indicates the loss of mitochondrial transmembrane potential (bottom).



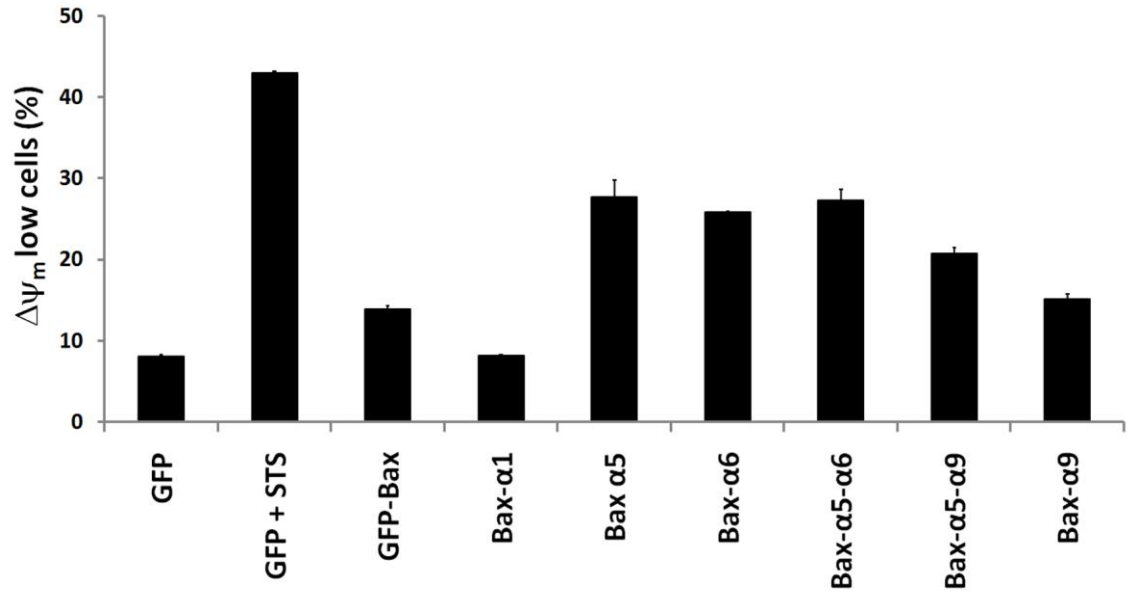
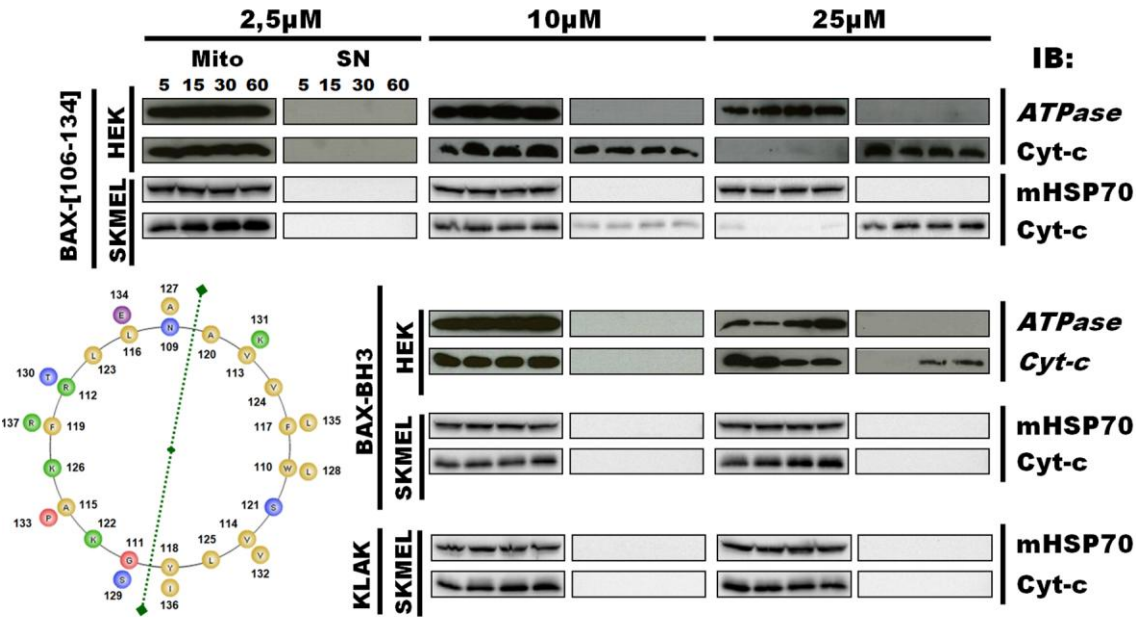
S3. Effect of synthetic Bax-derived peptides on isolated mitochondria.

Crude mitochondria were prepared from SK-MEL-28 and HEK 293T cells. In brief, cells were mechanically broken one time using a 2 ml glass/glass Dounce homogenizer (Kontes) (30 strokes). Homogenates were cleared at 1,500 g and mitochondria were spun down at 10,000 g. For cytochrome c release assays, 30 µg of crude mitochondria were resuspended at 1 mg/ml in KCl buffer supplemented with succinate (5 mM) and EGTA (0.5 mM). Peptides (2.5, 10 and 25 µM) were added to the samples and incubations were carried out at 30°C under agitation (300 rpm). At the indicated time points, samples were centrifuged (5 min, 10,000 g, 4°C); supernatants and pellets were recovered and analyzed by immunoblotting for cytochrome c and ATPase (subunit 6) or mitoHsp70.

(A) Cytochrome c release assays for the Bax[106-134] peptide using mitochondria isolated from SK-MEL-28 (upper panels) or HEK293T cells (lower panels). Results of the assays for the Bax BH3 and (KLAKLAK)₂ peptides are also shown. Peptides were incubated with isolated mitochondria for the indicated time periods (min) and the release of cytochrome c was monitored by immunoblotting (IB). MitoHSP70 or ATPase (subunit 6) was used as an equal-loading control for the pellet fraction. Control lanes indicate that in the preparation the MOM is intact and cytochrome c is retained within the intermembrane space. *Inset*: Helical wheel projection of the Bax[106-134] peptide. This amphipathic peptide includes the first helix (α5) of the pore-forming hairpin domain, the inter-helical residues previously implicated in the addressing and insertion of Bax into the mitochondrial membrane (Bellot et al., 2007), and the first amino acids of the second helix (α6) (Garcia-Saez et al., 2005; Garcia-Saez et al., 2006). Negatively charged residues are shown in purple, positively charged residues in green, polar residues in blue and hydrophobic amino acids in yellow. Numbers indicate amino acid positions in the native Bax protein.

(B) Bax[106-134]-induced mitochondrial swelling (left) and ΔΨ_m loss (right). Mitochondrial swelling and ΔΨ_m dissipation were measured using liver mitochondria as previously described (Jacotot et al., 2006). From that study, it appears that Bax[106-134] is a more potent inducer of mitochondrial swelling (SD50 = 3.98 ± 0.57 µM) and ΔΨ_m loss (DD50 = 1.68 ± 0.39 µM) than Bax-BH3 (SD50 > 200 µM; DD50 > 200 µM). NT = non-

1 treated.



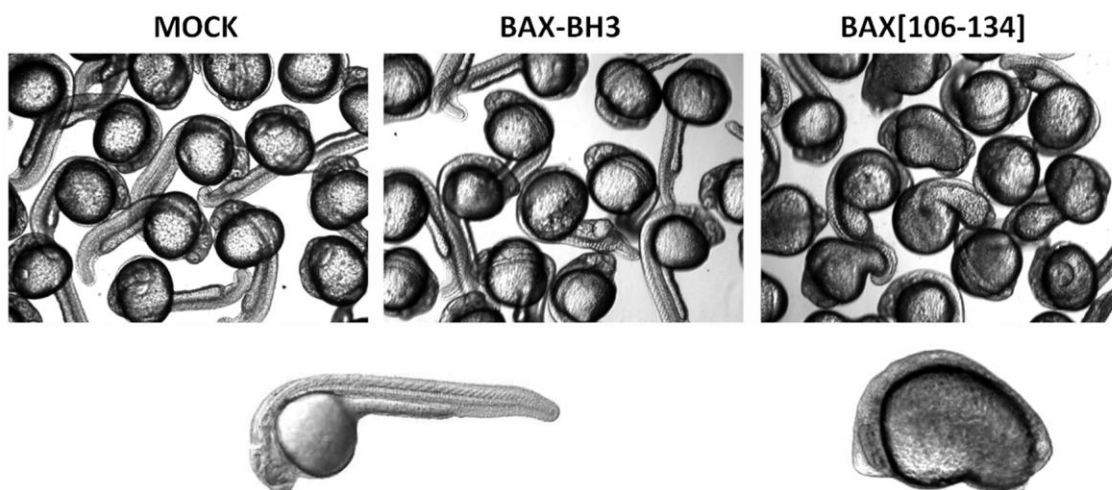
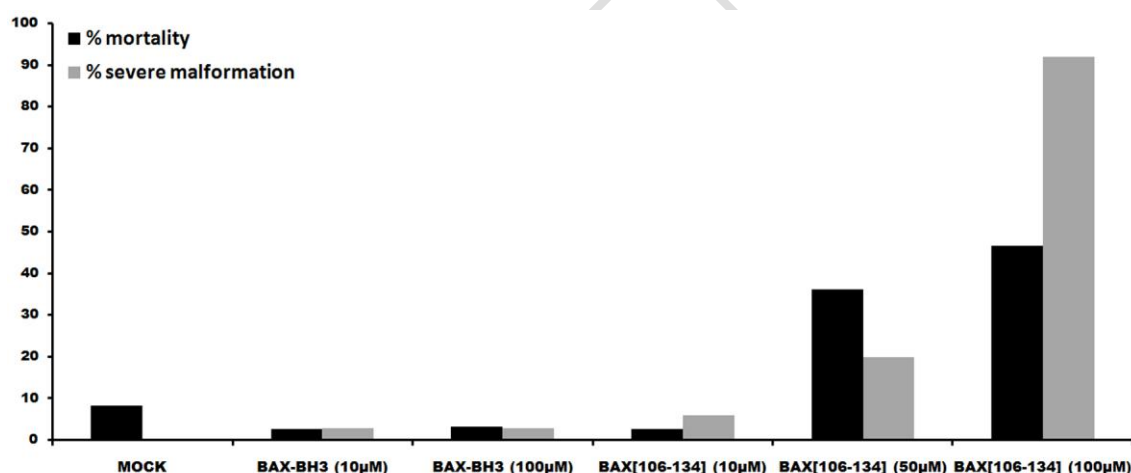
S4. Poro peptide-Bax[106-134] is toxic upon microinjection into zebrafish eggs.

The zebrafish system is a useful cellular model because (i) its apoptotic machinery is similar to the one of mammals, (ii) it is easier in principle to inject peptides into zebrafish eggs than in mammalian cells and (iii) it allow testing *in ovo* toxicity and possible developmental defects. Peptides (Bax[106-134] and Bax-BH3) were injected (~10 nL) into 1–2 cell stage *Danio rerio* embryos at 10, 50 and 100 μM. Ultrapure water was injected as a negative control. About 80 embryos were injected per condition. Zebrafish embryos were maintained at 28°C in 30% Danieau solution (58 mM NaCl, 0.7 mM KCl, 0.4 mM MgSO₄, 0.6 mM

Ca(NO₃)₂, 5 mM Hepes, pH 7.6). The egg morphology was observed 24h after the initial injection.

(A) Zebrafish eggs were microinjected at the 1-2 cell stage embryos with synthetic Bax[106-134] and Bax-BH3 peptides at 10, 50 and 100 μM (this later concentration corresponding to around 6x10¹² molecules of peptide per egg) or ultrapure water ('mock'). Histograms represent the percentage of mortality at 24h post fertilization and the percentage of embryos with severe malformations among the surviving embryos. Data are from a representative experiment repeated twice with similar results. Embryos microinjected with 10, 50 or 100 μM (in the injection capillaries) of Bax[106-134] showed 2%, 36% and 47% mortality at 24h, respectively. On the other hand, at the doses assayed, Bax-BH3 was ineffective in triggering specific embryonic death after microinjection in zebrafish eggs.

(B) Embryo morphology 24h after injection. Severe morphological malformations are observed in the group injected with Bax[106-134] compared to the group injected with Bax-BH3. Peptide concentration in the microinjection capillaries was 100μM. Note that all surviving embryos exhibited major malformations.

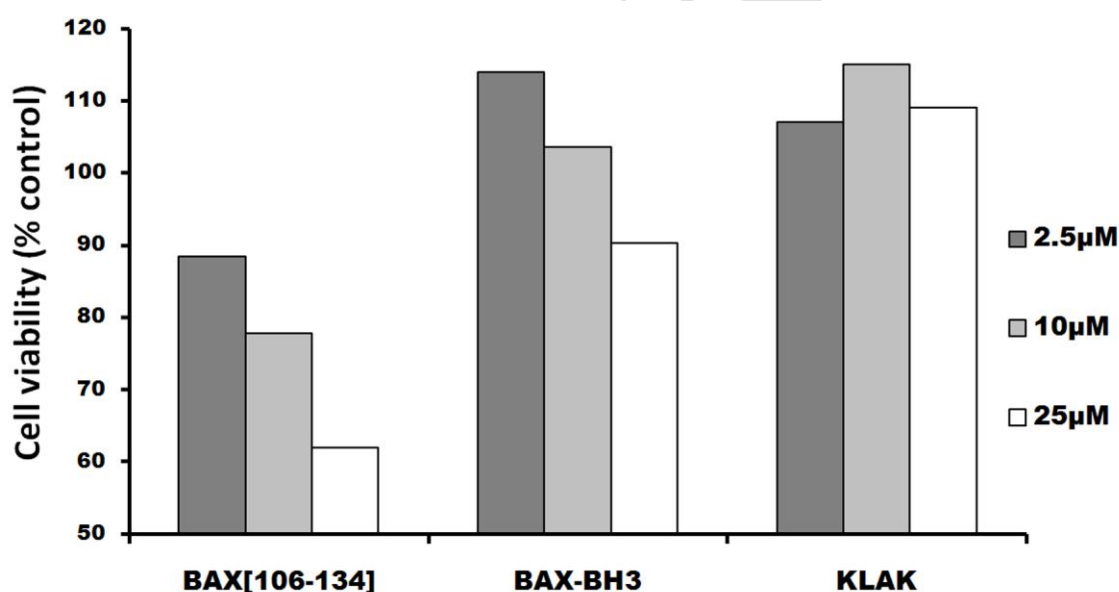
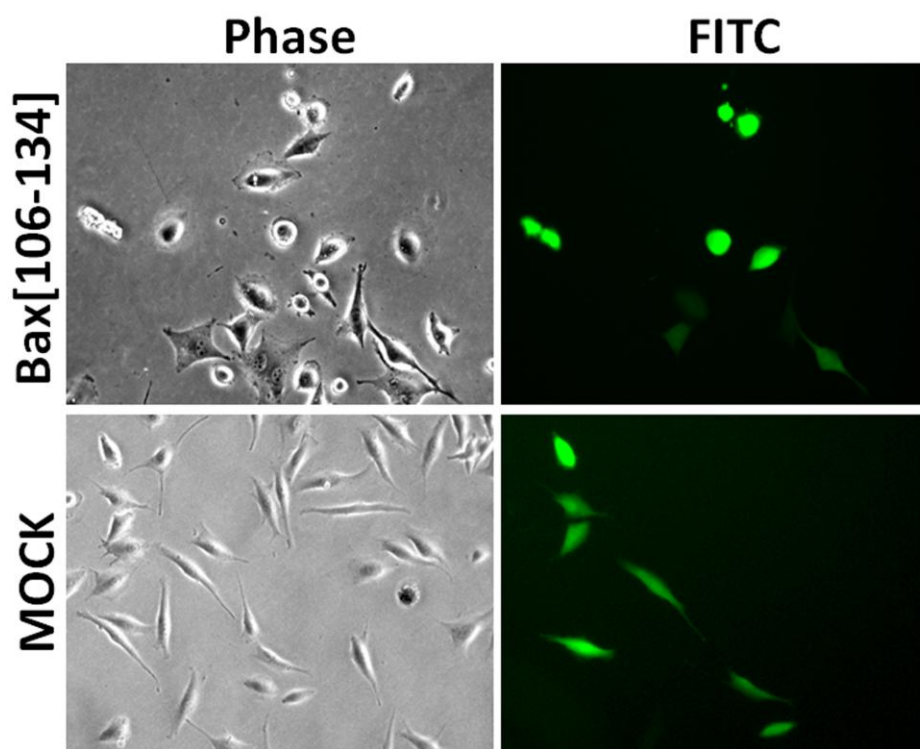


S5. Poro peptide-Bax[106-134] is toxic upon microinjection into human cancer cells.

Cytosolic microinjection was performed under a Nikon Eclipse TE200 inverted microscope using an Injectman NI2 (Eppendorf) and microinjector/micromanipulator Femtojet (Eppendorf). Cells were microinjected by using sterile microcapillaries (Femtotips, Eppendorf) loaded by sterile microloaders (Eppendorf). SK-MEL-28 cells were seeded on glass cellocate coverslips (Eppendorf) in 8 cm² dishes 20h prior to microinjection. An average of 100 cells per dish were injected with peptide solutions at different concentrations (2.5 μ M, 10 μ M and 25 μ M) in sterile buffer (Hepes 25 mM, CaCl₂ 8 mM, pH=7.4) and containing dextran conjugated Alexa Fluor 488 (10,000 MW, anionic, fixable, Molecular Probes). Control injections were done with dextran-conjugated Alexa Fluor 488 alone in buffer. All experiments were performed at an initial pressure of 85 Hpa for 0.2 seconds and a compensation pressure of 30 Hpa. The estimated injected volume into the cytoplasm is about 5 pl. Cells were moved into fresh medium immediately after microinjection and counted at various times (2, 8 and 24 h) using fluorescence microscopy.

(A) Microphotographs of SK-MEL-28 cells coinjected with FITC-dextran (mock) and Bax[106-134] and visualized by epifluorescence microscopy 12h after microinjection. These cells exhibited cytoplasmic blebbing and budding, which was not observed in cells microinjected with FITC-Dextran alone. Magnification, \times 800.

(B) Cell viability after microinjection of Bax[106-134], Bax-BH3, (KLAKLAK)₂ or R8 synthetic peptides. All microinjections were visualized by coinjection of FITC-labeled dextran. Cell death of SK-MEL-28 cells was determined from morphological alterations (cell shrinkage and round-up) 12h after microinjection. Data are from a representative experiment repeated twice with similar results. The Bax[106-134] peptide induced substantial cell death. In contrast, Bax-BH3, (KLAKLAK)₂ or R8-treated cells showed no significant difference from control cells.



S6. Peritumoral administration of Cy5-labeled poropeptide-Bax[106-134] in mammary adenocarcinoma (TS/A-pc) tumor-bearing athymic nude mice. Fluorescence Reflectance Imaging.

Female NMRI nude mice (6-8 weeks old, Janvier, Le Genest-Saint-Isle, France) were injected subcutaneously with mouse TS/A-pc cells (10^6 cells per mouse). After tumor growth (10 days), anesthetized mice (isoflurane/oxygen 4% for induction and 1.5/2% thereafter, CSP, Cournon, France) were injected peritumorally with 100 μ L of Cy5-Bax[106-134] suspension (300 nM of dye). Mice were illuminated by 633-nm light-emitting diodes equipped with

interference filters. Fluorescence images as well as black and white pictures were acquired by a back-thinned CCD camera (ORCAII-BT-512G, Hamamatsu, Massy, France) (Jin et al., 2006) fitted with a colored glass long-pass filter RG 665 (Melles Griot, Voisins Le Bretonneaux, France). At the end of the experiment, mice were euthanized to monitor peptide biodistribution in the different organs.

(A) Fluorescence reflectance imaging of athymic nude mice bearing subcutaneous TS/A-pc mammary adenocarcinoma tumor (right inferior limb) laid on the back, 1h (upper panel) and 24h (bottom panel) after peritumoral injection of Cy5-Bax[106-134] (representative example, N = 2).

(B) Corresponding peptide biodistribution data. Representative images of dissected organs (directly exposed under the camera) of mice sacrificed 24hrs p.i. The examined organs (arranged 4 by 4) are as follows: heart, lung, brain, skin, skeletal muscle, kidney, adrenal gland, urinary bladder, small intestine, spleen, pancreas, fat, stomach, uterus/ovary, liver, tumor. Upon peritumoral administration, the dye-conjugated peptide was mainly taken up by the tumor tissue, which exhibited strong Cy5 fluorescence intensity even 24h post-injection. These fluorescence data suggest that the Cy5-labeled ‘poropeptide’ has a sustained localization within the tumor micro-environment following peritumoral injection.

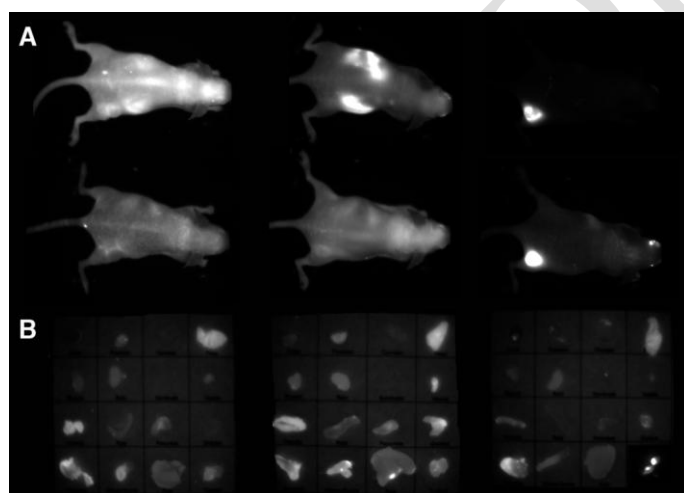


Table S1. Sequence of oligonucleotide primers used for this study.

Amino acid sequences of the peptides used in this study. MI = microinjection, CR = cytochrome c release, MSD = mitochondrial swelling and depolarization, CV = cell viability, ITA = antitumoral activity, IVB = in vivo biodistribution.

Peptide	Sequence	Length	Use
Bax[106-134]	NWGRVVALFYFASKLVLKALSTKVPELIR	29	CR, MI, MSD
Bax-BH3	VPQDASTKKLSECLKRIGDELDSNMELQR	29	CR, MI

KLAK	KLAKLAKKLAKLAK	14	CR, MI
R8-Bax[106-134]	FITC-RRRRRRRRGNWGRVVAlFYFASKLVlKALCTKVPElIR	38	CV, ITA
R8-Bax[Scr]	FITC-RRRRRRRRGLWSVPLVELAFANTASYGIRLKFKLVlRVK	38	CV, ITA
Cy5-Bax[106-134]	Cy5-NWGRVVAlFYFASKLVlKALSTKVPElIR	29	IVB

1

CONFIDENTIAL